Importin-β negatively regulates multiple aspects of mitosis including RANGAP1 recruitment to kinetochores

Emanuele Roscioli,[1] Laura Di Francesco,[2] Alessio Bolognesi,[1] Maria Giubettini,[1] Serena Orlando,[1] Amnon Harel,[3] Maria Eugenia Schininà,[2] and Patrizia Lavia[1]

[1]Institute of Molecular Biology and Pathology, CNR National Research Council, 00185 Rome, Italy
[2]Department of Biochemical Sciences, Sapienza University of Rome, 00185 Rome, Italy
[3]Department of Biology, Technion-Israel Institute of Technology, Haifa 32000, Israel

Importin-β is the main vector for interphase nuclear protein import and plays roles after nuclear envelope breakdown. Here we show that importin-β regulates multiple aspects of mitosis via distinct domains that interact with different classes of proteins in human cells. The C-terminal region (which binds importin-α) inhibits mitotic spindle pole formation. The central region (harboring nucleoporin-binding sites) regulates microtubule dynamic functions and interaction with kinetochores. Importin-β interacts through this region with NUP358/RANBP2, which in turn binds SUMO-conjugated RANGAP1 in nuclear pores. We show that this interaction continues after nuclear pore disassembly. Overexpression of importin-β, or of the nucleoporin-binding region, inhibited RANGAP1 recruitment to mitotic kinetochores, an event that is known to require microtubule attachment and the exportin CRM1. Co-expressing either importin-β–interacting RANBP2 fragments, or CRM1, restored RANGAP1 to kinetochores and rescued importin-β–dependent mitotic dynamic defects. These results reveal previously unrecognized importin-β functions at kinetochores exerted via RANBP2 and opposed by CRM1.

Introduction

Importin-β is the main vector for protein import in interphase nuclei (Harel and Forbes, 2004; Mosammaparast and Pemberton, 2004). It acts mainly in association with importin-α family members, which recognize protein cargoes bearing nuclear localization signals (NLSs), to assemble import complexes (importin-β–importin-α–NLS cargo) in the cytoplasm. In some cases, importin-β interacts directly with cargoes without the mediation of an importin-α member. Importin-β then translocates the import complex through nuclear pore complexes (NPCs), with which it interacts via nucleoporin (NUP)-binding sites. In the nucleus, importin-β is bound by the GTPase RAN, converted into RANGTP by the chromatin-bound GTP exchange factor RCC1: this dissociates the import complex and releases cargoes within the nucleus. RANGTP and importin-β then exit the nucleus and dissociate in the cytoplasm, aided by hydrolyzing factors for RAN, i.e., the GTPase-activating protein RANGAP1 and its cofactor RANBP1.

Nuclear import depends on the ability of importin-β domains to establish distinct interactions in different subcellular compartments (Cingolani et al., 1999; Vetter et al., 1999; Bayliss et al., 2000, 2002). The C-terminal region, containing an importin-α–binding domain (IAB), hence indirectly interacting with NLS proteins, is essential for import complex assembly in the cytoplasm. An extended central region harbors binding sites for phenylalanine/glycine (FG) and FxFG repeats in NUPs, which enables importin-β to traverse the NPC along with import cargoes (Ben-Efraim and Gerace, 2001). There is partial overlap

Correspondence to Patrizia Lavia: patrizia.lavia@uniroma1.it

E. Roscioli's present address is Dept. of Biological Sciences, Virginia Tech, Blacksburg 24060, VA.

A. Bolognesi's present address is Institut für Biochemie, ETH Zürich, 8093 Zürich, Switzerland.

S. Orlando's present address is Faculty of Medicine, University of Barcelona, 08036 Barcelona, Spain.

Abbreviations used in this paper: FG, phenylalanine/glycine; IAB, importin-α–binding domain; IF, immunofluorescence; IP, immunoprecipitation; KT, kinetochore; MT, microtubule; NE, nuclear envelope; NLS, nuclear localization signal; NPC, nuclear pore complex; NUP, nucleoporin; SAC, spindle assembly checkpoint; WB, Western blot; XEE, *Xenopus* egg extract.

The Rockefeller University Press $30.00
J. Cell Biol. Vol. 196 No. 4 435–450
www.jcb.org/cgi/doi/10.1083/jcb.201109104

between the NUP-binding and the RAN-binding regions. The most N-terminal region binds RANGTP and is indispensable for cargo release in the nucleus. Thus, importin-β domains are organized with an intrinsic functional "polarity" that parallels the directionality of the import process (Ström and Weis, 2001).

Importin-β also has roles after nuclear envelope (NE) breakdown (Ciciarello et al., 2007; Clarke and Zhang, 2008; Kalab and Heald, 2008): it inhibits NLS-containing mitotic factors that interact with it, until RANGTP binding to importin-β releases these factors free to function in spindle organization. This model has clear mechanistic analogy with that governing nuclear import and has received ample experimental confirmation in studies with *Xenopus* egg extracts (XEEs; Gruss et al., 2001; Nachury et al., 2001; Wiese et al., 2001). The small volume of mammalian mitotic cells, however, imposes spatial constraints for the spindle organization and function, which XEEs cannot fully recapitulate (Roscioli et al., 2010), calling for specific studies of importin-β modes of action in mitotic somatic cells.

In early studies, importin-β protein microinjection into rat kangaroo kidney Ptk cells was found to cause disorganized mitotic spindles and misaligned chromosomes (Nachury et al., 2001). In human cells, importin-β interacts with mitotic microtubules (MTs) and accumulates at spindle poles (Ciciarello et al., 2004), where a RANGTP fraction also colocalizes (Tedeschi et al., 2007). Moderate importin-β overexpression induced multipolar spindle formation, visible in fixed and stained HeLa cells, with no obvious disruption of nuclear functions or transport (Ciciarello et al., 2004). Spindle pole integrity was restored by coexpressing TPX2 (Ciciarello et al., 2004), an NLS-bearing factor with spindle pole–organizing and MT-regulatory activities (Gruss and Vernos, 2004). These data demonstrated that NLS factor inhibition by importin-β is a conserved mechanism and, in addition, introduced the notion that importin-β operates in physical association with the mitotic spindle in human cells.

Studies in human cells also pinpointed roles of RAN at kinetochores (KTs), in both the nucleation of KT-originated MTs during spindle assembly (Tulu et al., 2006; Torosantucci et al., 2008; Mishra et al., 2010) and in the establishment of interactions between MTs and KTs (Arnaoutov and Dasso, 2003; Arnaoutov et al., 2005). Importin-β negatively regulates KT-driven MT nucleation by inhibiting factors such as TPX2 (Tulu et al., 2006) and HURP (Torosantucci et al., 2008), but it has not been implicated in MT–KT interactions thus far. Instead, fractions of RANGAP1 and RANBP2 (also known as NUP358) are identified at KTs after MT attachment (Joseph et al., 2004; Dasso, 2006). RANBP2 is a large NUP, harboring many FG and FxFG repeats with which importin-β interacts during import complex translocation across interphase NPCs (Ben-Efraim and Gerace, 2001; Bayliss et al., 2002; Bednenko et al., 2003). RANBP2 also has E3 SUMO-ligase activity (Pichler et al., 2002) and targets SUMO-conjugated RANGAP1 to NPCs, possibly to clear NPCs of RANGTP and prevent premature import complex dissociation (Mahajan et al., 1998; Matunis et al., 1998). After NE breakdown RANBP2 has complex mitotic roles, as its inactivation yields spindle pole fragmentation, chromosome misalignment, and unstable K-fibers (Salina et al., 2003; Joseph et al., 2004; Dawlaty et al., 2008; Klein et al., 2009; Hamada et al., 2011). RANBP2 remains associated with SUMO–RANGAP1 after NPC disassembly (Swaminathan et al., 2004) and targets it to KTs after MT attachment (Joseph et al., 2002, 2004). This localization requires RANGTP and exportin-1/CRM1 (Arnaoutov et al., 2005), the vector for protein nuclear export. A self-regulatory loop can thus take place at each mitotic cycle, whereby RANGTP accumulates at chromosomes under the continuous activity of RCC1; when MTs attach to KTs, RANGTP, in concert with CRM1, recruits SUMO–RANGAP1 and activates the hydrolysis of its bound nucleotide at KTs (Dasso, 2006). These data suggest that RAN operates with distinct modes along the spindle, where it counteracts importin-β and releases active NLS-containing spindle-organizing factors, and at KTs, where it cooperates with CRM1 in recruiting factors that eventually determine its own hydrolysis. Despite these advances, much remains to be learned on how these mechanisms integrate in a normal mitotic progression.

Here we show that importin-β uses distinct domains to regulate diverse aspects of mitosis in human cells, including spindle pole formation, chromosome alignment, mitotic progression, and RANGAP1 localization at KTs. Moreover, importin-β and CRM1 regulate in opposite manners the delivery of RANGAP1 to MT-attached KTs. Importin-β therefore emerges as a global regulator in multiple steps of mitotic progression.

Results

Overexpression of importin-β induces mitotic dynamic defects in HeLa cells

To extend our previous findings that importin-β regulates spindle pole formation in human cells (Ciciarello et al., 2004), we transfected HeLa cells with an importin-β construct, then synchronized cell cultures by S phase block and release and followed them during synchronous cell cycle progression. In the presence of moderate importin-β overexpression (two- to threefold average increase, with variations in single transfected cells; Fig. S1), cells pass the G2/M transition normally with no visible disruption of nuclear shape, cytoskeleton organization, cell viability, or cell cycle checkpoint controls elicited by S phase synchronization protocols. We recorded importin-β–overexpressing cells while undergoing the first mitosis after release of S phase arrest by time-lapse imaging. HeLa cells take ∼2 h to progress from NE breakdown to daughter nuclei reformation (Fig. 1 A; Video 1). A fraction of importin-β–transfected cells undergo multipolar divisions (Fig. 1 B; Video 2), consistent with our previous findings in fixed cells (Ciciarello et al., 2004). Somewhat unexpectedly, most importin-β–transfected cells developed diversified defects other than multipolar division (Table 1). A fraction showed significant prometaphase and metaphase delay and some never progressed past those stages for the entire duration of the video. Chromosome alignment was often unstable and alternated with redispersal in a broader plate resembling prometaphase (Fig. 1 C; Video 3). These abnormal movements went on in repeated cycles (for example, in Fig. 1 C, note the alignment at 68 and 322 min, followed by redispersal at 278 and 352 min, before alignment is eventually stabilized). In some cases, some chromosomes never reached congression, but remained

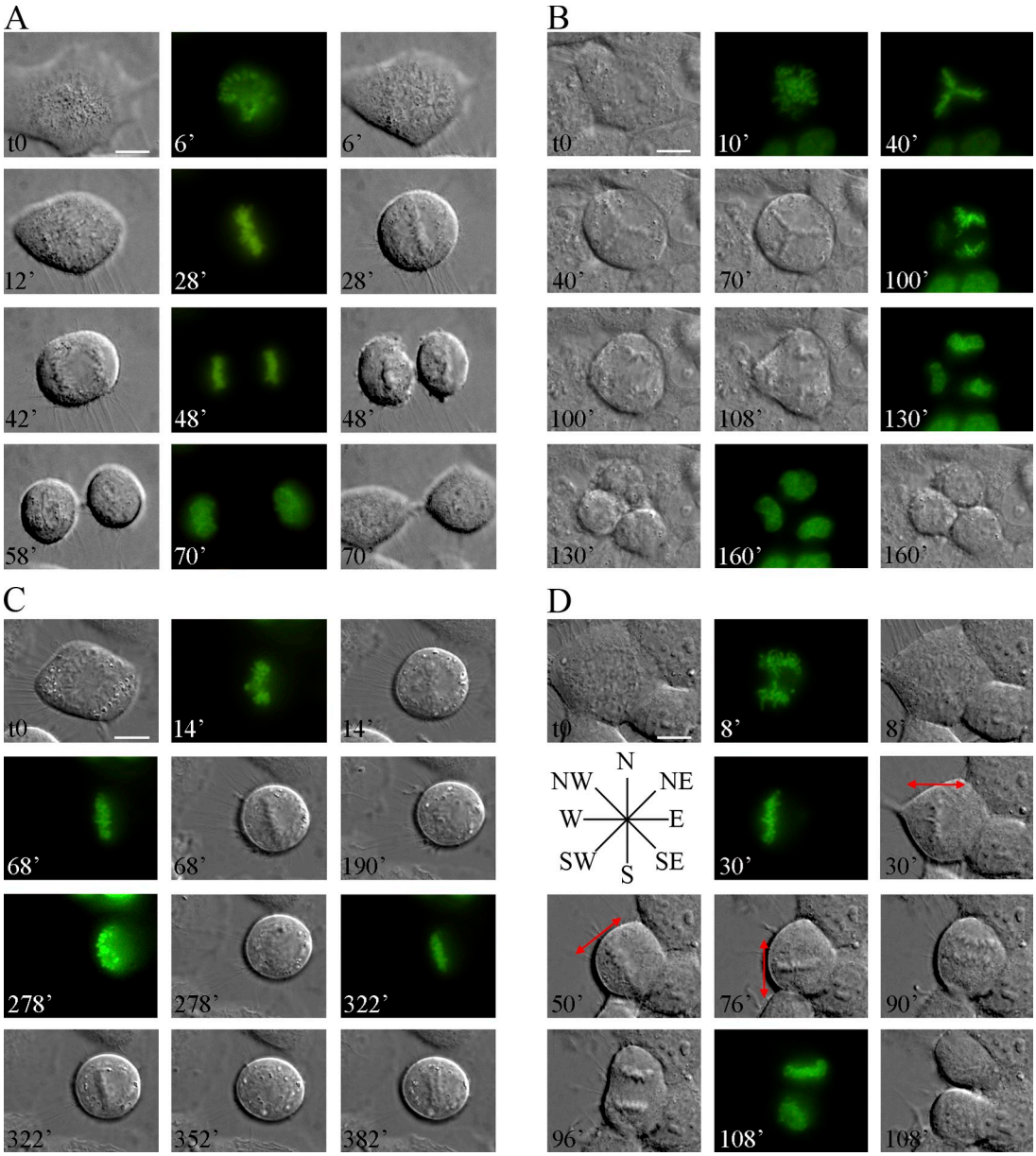

Figure 1. **Mitotic abnormalities in video-recorded importin-β–overexpressing HeLa cells.** (A) A mitotic HeLa cell transfected with vector and H2B-GFP construct to visualize chromosomes (Video 1). (B) A tripolar mitosis transfected with importin-β 1–876 and H2B-GFP; chromosomes segregate into three unequal masses (Video 2). (C) An importin-β–transfected cell in which chromosomes align at the equator (68 min), then lose alignment (278 min), then reach alignment again (322 min), lose it (352 min), and eventually align stably (382 min) before segregation (Video 3). (D) An importin-β–transfected mitosis displaying unstable positioning of the spindle axis (double-arrowed red line). The spindle undergoes extensive rotation (30- to 76-min panels) before the onset of segregation (Video 4). All images were taken under an inverted microscope (Ti Eclipse, Nikon; DIC frames every 2 min, fluorescence frames every 20–30 min). Bars, 10 µm.

near one pole throughout the recording time, and lagging chromosomes were visible in anaphase. We also recorded cells in which chromosomes congressed, but then the spindle underwent extensive reorientation during prolonged metaphase (Fig. 1 D; Video 4). These defects were recorded in importin-β–transfected cells with normal bipolar spindles and they are therefore independent of the induction of multipolar spindles. Most recorded defects could not have been diagnosed by immunofluorescence (IF) in fixed cells: for example, in Fig. 1 C the 68-min panel would classify as a normal metaphase and the 278-min panel as a prometaphase, and it is only the imaging sequence that reveals an abnormal progression. Similarly, the metaphase panels in Fig. 1 D look normal in isolation, yet their sequence reveals an unstable spindle positioning. To simplify our analysis, we grouped the phenotypes that would have escaped notice in fixed cells under the broad category of dynamic defects, as opposed to structural defects affecting the spindle shape and/or involving multipolar chromosome distribution, which would also have been detected in fixed cells (e.g., Fig. 1 B). Thus, importin-β overexpression induces a broader variety of mitotic defects than previously identified in fixed cells, mostly of a dynamic nature.

Table 1. **Mitotic phenotypes in cells overexpressing wild-type importin-β**

Recorded phenotypes	*n*	%	Categories
Multipolar division	4	10.53	Structural
Abnormal chromosome alignment	2	5.26	Structural
PM/M arrest/delay	10	26.32	Dynamic
Chromosome oscillation in PM/M and arrest	2	5.26	Dynamic
Chromosome oscillation in PM/M and delay	4	10.53	Dynamic
Spindle axis reorientation	3	7.89	Dynamic
Total abnormal cells	25	65.79	
Total recorded cells	38		

PM, prometaphase; M, metaphase.

Importin-β generates distinct mitotic phenotypes through specific domains

To understand how importin-β overexpression generates mitotic defects, we expressed importin-β mutants lacking specific domains (Fig. S1 A). The N-terminal 1–44 deletion, though not removing the entire RAN-binding domain, is sufficient to prevent RAN binding in HeLa cells (Ciciarello et al., 2010), rendering the 45–876 mutant refractory to cargo release modulation by RANGTP. Removal of the 463–876 region prevents importin-α binding and hence the formation of complexes with NLS factors. The 45–462 double deletion mutant retains NUP-binding sites. These mutants play distinct roles in nuclear import assays in permeabilized HeLa cells (Kutay et al., 1997). In addition, we generated a full-length site-specific mutant in two critical residues (I178 and Y255) required for the interaction with FG-NUPs (Bayliss et al., 2000; Bednenko et al., 2003; see Fig. 5 E). All constructs are similarly expressed in HeLa cells (Fig. S1).

IF analysis (Fig. 2) revealed spindles with abnormal poles in cells overexpressing importin-β 1–876, or site-specific mutant I178A/Y255A or the N-deletion 45–876. The induction of multipolar spindles was statistically significant compared with that scored in cultures transfected with either pEGFP, or H2B-GFP or wild-type RCC1, which, when overexpressed, affects the spindle organization only mildly if at all, unlike chromatin localization-defective RCC1, which has disruptive effects (Moore et al., 2002; Chen et al., 2007).

Importin-β mutants lacking the C-terminal domain, i.e., 1–462 and 45–462, yielded fewer spindle pole defects, but chromosome arrangements were often abnormal (Fig. 2 A, arrows): chromosomes failed to align in metaphase (suggestive of syntelic or monotelic attachments); in addition, lagging chromosomes were observed in anaphase and chromatin bridges in telophase (suggestive of merotelic attachments). Comparable results were induced by either GFP-tagged or untagged importin-β derivatives (Fig. 2 A). Thus, abnormalities in spindle pole organization in importin-β–overexpressing cells depend on the integrity of the C-terminal region, which contains the IAB, whereas chromosome alignment defects are not dependent on this region.

Time-lapse imaging of cells transfected with the same mutants revealed a more diversified scenario. None of the mutants affected cell cycle progression before mitosis: cells passed regularly through the G2/M transition after release from S phase arrest; NE breakdown was normal and prophase unfolded regularly up to the point where centrosomes separate and begin to nucleate MT asters. At this point individual importin-β mutants generated specific defects. Cells overexpressing mutant 45–876 showed a similar array of defects than with wild-type importin-β, but with higher frequency (Table 2). Cells transfected with importin-β 45–462, although developing few spindle structural defects in fixed cells, displayed the highest frequency of dynamic defects, e.g., unstable chromosome alignment, abnormal oscillations at the equator, and spindle axis rotation (Table 2; Fig. 3). The 45–462 mutant also severely prolonged prometaphase and metaphase (Fig. 4 B). Silencing of Mad2, a major spindle assembly checkpoint (SAC) effector (Fig. 4 A), abolished that delay (Fig. 4 B) and induced rapid progression to anaphase with incorrect chromosome segregation (Fig. 4 C). Because importin-β does not influence the SAC activity (Arnaoutov and Dasso, 2003), these results suggest that the dynamic abnormalities induced via the 45–462 region maintain the SAC active, causing prolonged prometaphase and metaphase. By contrast, cells expressing importin-β I178A/Y255A displayed a significantly lower frequency of misaligned, misoriented, or lagging chromosomes (grouped as dynamic defects in Table 2). Thus, importin-β regulates as diverse processes as the spindle pole organization through the IAB, versus chromosome alignment and mitotic progression through the NUP-binding region.

Importin-β, RANBP2, and SUMO-RANGAP1 interact in mitotic cells after NPC disassembly

To identify potential partners implicated in importin-β–dependent mitotic dynamic defects, we immunoprecipitated importin-β from mitotic cells collected by shake-off and analyzed coimmunoprecipitation (coIP) partners by mass spectrometry. Part of the mitotic sample was replated to allow cells to terminate mitosis and reenter interphase to compare to well-characterized interphase interactions (Fig. 5 A). We found both RANBP2 and SUMO-conjugated RANGAP1 in the mitotic coIP (Fig. 5 B; details in Table S1). Although SUMO-conjugated RANGAP1 forms were less abundant in extracts prepared in coIP buffer compared with denaturing conditions, suggesting that some desumoylating activities were active in the former (Fig. 5 C), Western blot (WB) analysis revealed quantitative segregation of SUMO–RANGAP1, including the mitosis-specific phosphorylated forms, with importin-β and RANBP2 (Fig. 5 D).

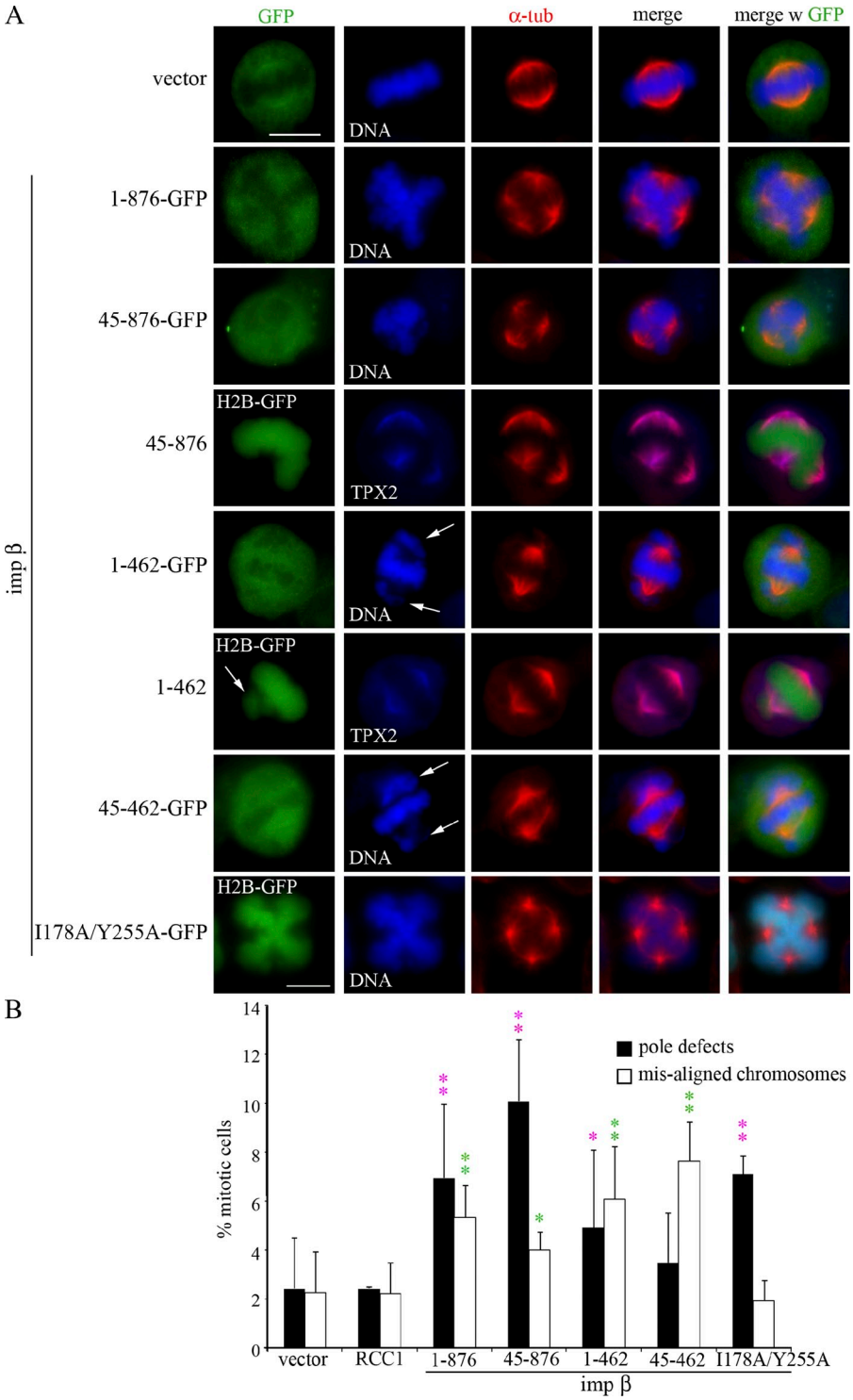

Figure 2. **Importin-β mutants cause distinct mitotic abnormalities in fixed HeLa cells.** (A) Mitotic cells transfected with pEGFP vector, or with GFP-tagged or untagged importin-β mutants, fixed and stained for either α-tubulin and DAPI, or for TPX2 to stain MTs; in that case chromosomes are visualized by H2B-GFP incorporation. Misaligned chromosomes in apparently normal bipolar mitoses are arrowed. Bars, 10 µm. (B) Quantification of mitotic defects induced by importin-β mutants in fixed cells. Means and standard deviations were calculated from 1,000–1,800 cells for most samples (5 to 10 experiments) and 500 cells for RCC1 (4 experiments). *, significant ($P < 0.05$); **, highly significant ($P < 0.01$) differences relative to vector (χ^2 test) are shown in purple (spindle pole defects) and green (misaligned chromosomes), respectively.

RANGAP1 that was not conjugated to SUMO (either phosphorylated in the mitotic sample or nonphosphorylated in interphase) was released in the supernatant. We conclude that the interaction of importin-β with RANBP2 and SUMO–RANGAP1 continues in mitosis and does not require NPCs as a physical platform.

We next analyzed the coIP of GFP-tagged importin-β derivatives in mitotic cell extracts using anti-GFP antibody (Fig. 5 E). A small fraction of RANBP2 was found in the coIP of both importin-β 1–876 and 45–462: thus, the isolated 45–462 region can compete with endogenous importin-β and act as a dominant-negative in mitotic cells. No trace of RANBP2 did instead coIP with mutant I178A/Y255A, which was still proficient for RAN binding.

Importin-β associates with spindle MTs at least in part via dynein (Ciciarello et al., 2004; Hughes et al., 2008). RANGAP1 and RANBP2 also associate with the spindle MTs, with a fraction reaching KTs after attachment (Joseph et al., 2002, 2004). To assess whether MTs, which represent a common location,

Table 2. **Recorded mitotic defects in cells transfected with importin-β derivatives**

Transfection[a]	Structural defects	Dynamic defects	Delay only	Recorded mitoses
	%	%	%	*n*
Control vector	6.45	3.23	6.45	31
Imp-β 1–876	15.79	28.95	21.05	38
Imp-β 45–876	23.53	41.18	26.47	34
Imp-β 45–462	11.76	54.90	21.57	51
Imp-β I178A/Y255A	33.33	3.70	18.52	54

[a]A trace of H2B-GFP was added to all transfection mixes.

are required for the interaction of importin-β with RANBP2/SUMO–RANGAP1 to take place, we compared the importin-β coIP from normal mitotic cells collected by shake-off after thymidine release to nocodazole-treated cells, in which MT assembly was prevented (Fig. 6 A). Cells were immediately extracted and processed for IP. In Fig. 6 B, effectively SUMO-conjugated RANGAP1 coIPed entirely with importin-β and RANBP2 in the presence and absence of MTs. A reciprocal RANBP2 IP experiment confirmed that importin-β was present in the coIP in either condition (Fig. 6 C). These data suggest that their association persists after NPC disassembly, whether or not mitotic MTs are present.

Overexpression of importin-β, or of the 45–462 region, hinders RANGAP1 recruitment to KTs

Importin-β and RANBP2/SUMO–RANGAP1 interact in cells collected by shake-off (mostly prometaphases; Fig. 5) and colocalize along the spindle MTs. A RANBP2/SUMO–RANGAP1 fraction is recruited onto KTs when MTs attach to them (Joseph et al., 2002, 2004), whereas importin-β remains MT-associated until mid-anaphase and thereafter relocalizes around segregating chromosomes (Ciciarello et al., 2004). We reasoned that overexpressed importin-β, which binds RANBP2 via the 45–462 region, might hinder RANBP2/SUMO–RANGAP1 recruitment onto KTs. To test this, we transfected cells with either full-length importin-β, or with the 45–462 mutant that can bind RANBP2, or with the I178A/Y255A mutant that cannot, then examined RANGAP1 localization. Many mitotic cells transfected with importin-β, and more significantly, with 45–462, showed KTs attached to MTs that were devoid of RANGAP1; RANGAP1 instead localized correctly at KTs in metaphase cells expressing importin-β I178A/Y255A (examples in Fig. 7 A, quantified in Fig. 7 B). Moreover, importin-β 1–876- or 45–462-expressing metaphase cells that did show some RANGAP1 at KTs (identified by CREST, Fig. 7 D) displayed significantly

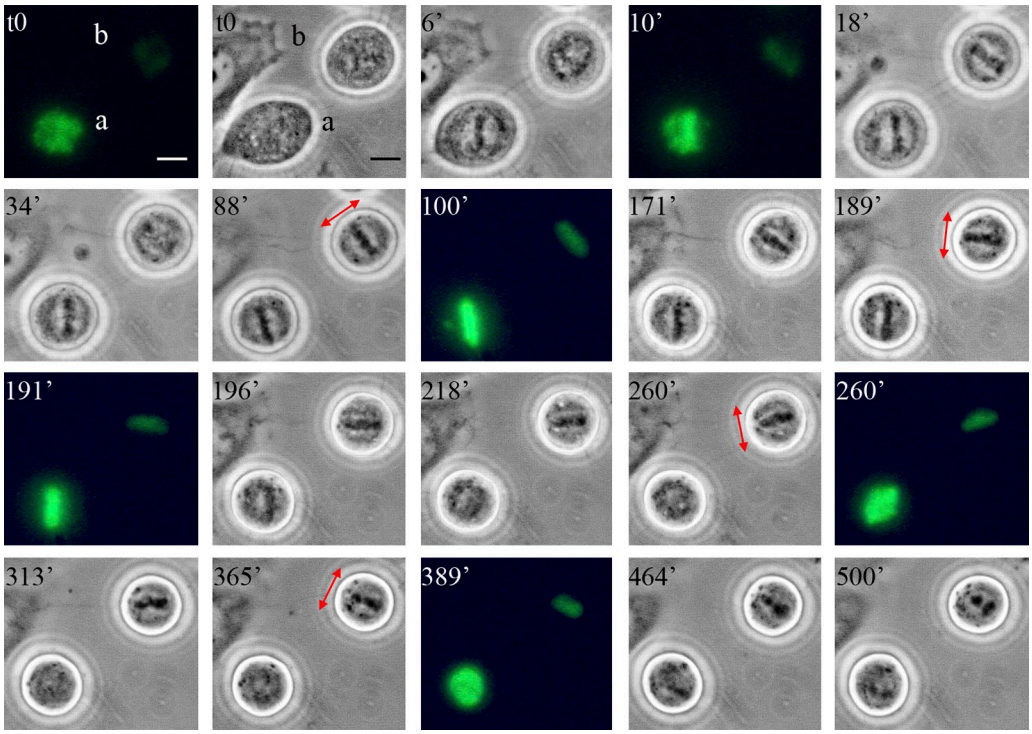

Figure 3. **Importin-β 45–462 induces mitotic dynamic defects in time-lapse recorded HeLa cells.** Still images from video-recorded cells transfected with importin-β 45–462 and H2B-GFP, displaying unstable chromosome alignment (cell a) and spindle axis rotation (cell b, the double-arrowed red line represents the major spindle axis). Images were taken under an inverted microscope (TE300, Nikon; wide-field channel every 2 min, fluorescence channel every 30 min). Bars, 10 µm.

A

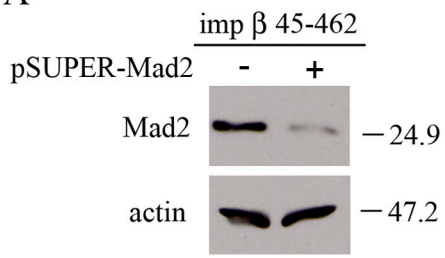

B **Timing of mitosis in cells transfected with importin β derivatives**

Transfected construct	Duration (min) PM	M	A	T	total	recorded cells (n)
Control vector	23.58	31.23	11.92	40.46	113.20	31
Imp β 1-876	47.25	66.39	11.67	36.85	162.16	41
Imp β 1-876/pSUPER-Mad2	16.64	2.73	7.44	24.56	51.36	11
Imp β 45-462	25.91	155.94	13.42	39.84	235.11	51
Imp β 45-462/pSUPER-Mad2	13.00	9.17	8.67	27.75	58.58	12

PM, prometaphase; M, metaphase; A, anaphase; T, telophase

C

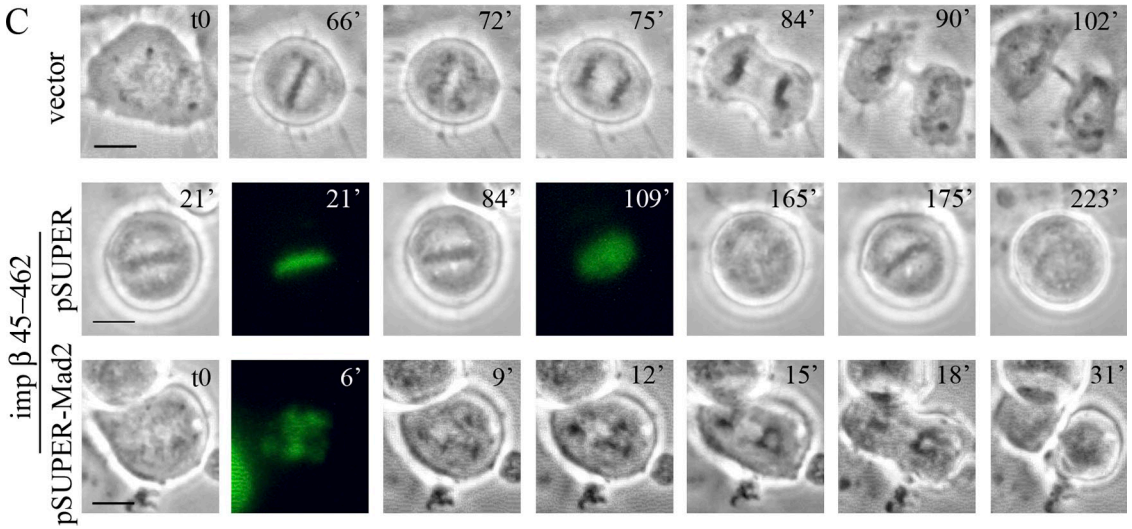

Figure 4. **Prolonged mitotic duration in importin-β 45–462-transfected cells requires Mad2 activity.** (A) WB analysis of Mad2 protein in cells collected by shake-off after cotransfection with importin-β 45–462 and either pSUPER vector (lane −), or pSUPER-Mad2, expressing Mad2-specific shRNAs (lane +). (B) The induction of mitotic delay in video-recorded cells transfected with importin-β 1–876 or 45–462 requires Mad2. (C) Examples of: (a) A vector-transfected cell, completing mitosis in ∼1.5 h; and of cells cotransfected with either importin-β 45−462 and pSUPER vector (b, note chromosome oscillations and prolonged duration); or with importin-β 45−462 and pSUPER-Mad2 (c), exiting mitosis in less than 1 h with abnormal chromosome segregation. Images were acquired as described for Fig. 3. Bars, 10 μm.

reduced recruitment compared with KTs of control cells in quantitative IF analysis (Fig. 7 C). Thus, importin-β inhibits RANGAP1 localization at KTs in a manner dependent on binding to NUPs.

CRM1 and RANGTP positively regulate RANGAP1 localization to KTs (Arnaoutov et al., 2005). We wondered whether the failure of RANGAP1 to localize at KTs was in fact caused by a primary defect in CRM1 localization in importin-β–overexpressing cells. CRM1 shows a typical IF pattern lining the outer KTs, as described previously (Arnaoutov et al., 2005), which was unaffected by importin-β overexpression (Fig. S2 A). CENP-F, a MT- and KT-associated factor that is recruited to KTs in a manner dependent on both RANBP2 (Salina et al., 2003; Joseph et al., 2004) and the NUP107/160 complex (Zuccolo et al., 2007) was instead altered, with a tight persistence at the spindle MTs and concomitantly reduced KT signals, in mitoses expressing full-length or 45–462 importin-β (Fig. S2 B). By contrast, neither full-length nor the 45–462 region of importin-β

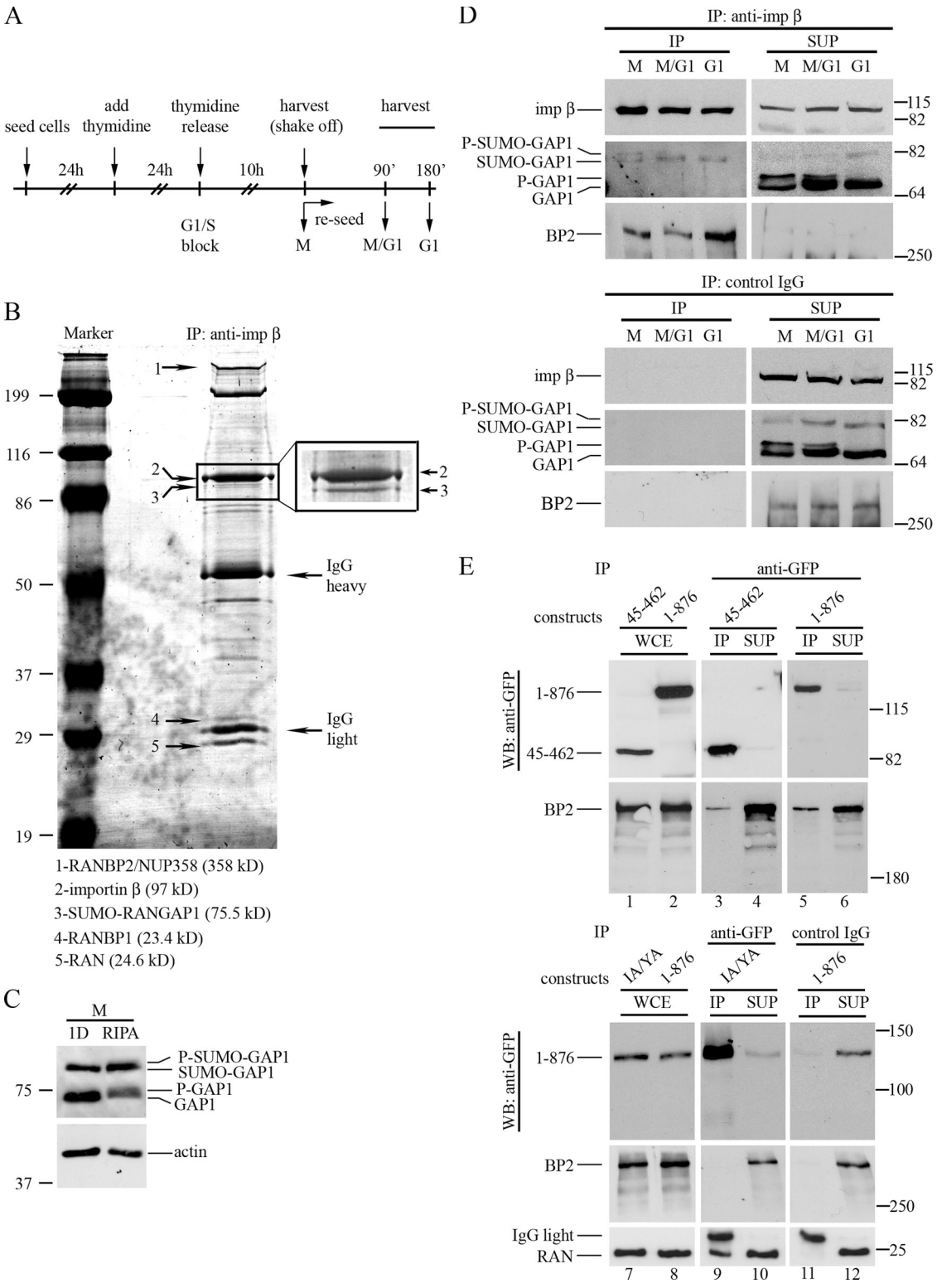

Figure 5. **Importin-β partners in coIP assays from HeLa cells.** (A) Synchronization protocol used for protein analysis. The mitotic shake-off sample (mostly prometaphases) was compared with cells collected at mitotic exit or in G1. (B) Coomassie blue–stained proteins in the importin-β coIP from HeLa mitotic cells (10% SDS-PAGE). Bands were excised and processed for mass spectrometry (Table S1). The inset shows an enlarged section from a parallel gel to resolve importin-β and SUMO–RANGAP1, which migrate very close. (C) RANGAP1 in cell extracts prepared either in RIPA or in nondenaturing (1D) buffer: note the reduced abundance of SUMO-conjugated forms in 1D buffer. (D) WB analysis of importin-β partners. Protein extracts were IPed using anti–importin-β antibody (top); importin-β partners are visible in the coIP pellet, noninteracting proteins are released in the supernatant (SUP). The bottom panel shows the same extract incubated with nonspecific IgG for control. (E) CoIP assays of importin-β constructs detected using GFP antibody. RANBP2 was identified in whole cell extracts (WCE) from mitotic cultures transfected with the indicated constructs (lanes 1–2 and 7–8) and in coIP together with importin-β 45–462 (lanes 3–4) and 1–876 (lanes 5–6), but not I178A/Y255A (lanes 9–10, indicated as IA/YA); the latter is functional for RAN binding. In parallel, importin-β 1–876-transfected WCE was IPed with nonspecific IgG (lanes 11–12).

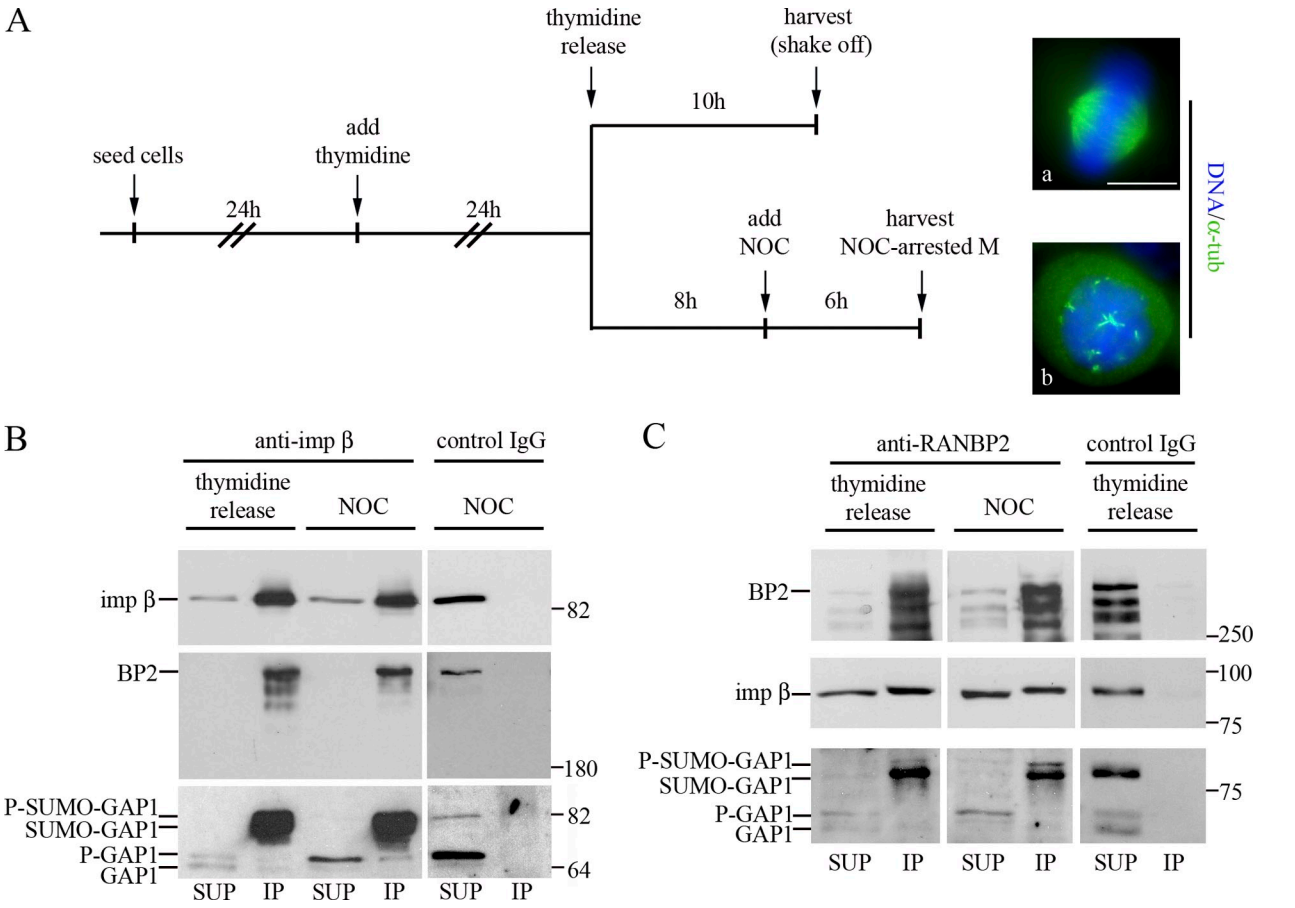

Figure 6. **Importin-β interacts with RANBP2 in normal and MT-lacking mitotic cells.** (A) Protocol for protein extract preparation from cultures reaching mitosis after thymidine release (a) or in the presence of nocodazole (NOC) to prevent MT polymerization (b). Bar, 10 µm. Protein extracts were prepared immediately after cell harvesting. (B) WB analysis of coIP proteins using anti–importin-β or nonspecific IgG for control. (C) Reciprocal analysis of proteins in the RANBP2 coIP and in cell extracts incubated with nonspecific IgG.

affected BUB1, which acts directly in the SAC but does not depend on RANBP2–RANGAP1 for KT localization (Fig. S3). Thus, an excess of importin-β neither hinders CRM1 localization nor alters the overall KT structure or ability to recruit SAC factors before MT attachment, but selectively delocalizes factors that depend on RANBP2 for localization to KTs.

Co-expression of RANBP2 or of CRM1 "rescues" importin-β–dependent abnormalities

The results thus far indicate that chromosome congression and alignment, mitotic progression, and RANGAP1 localization at KTs are impaired in cells overexpressing importin-β, and particularly 45–462, which binds RANBP2, but not importin-β I178A/Y255A, which is unable to do so. This suggests that a regulated balance exists between the importin-β–bound and the KT-bound RANBP2–RANGAP1 complexes before and after MT attachment, and that increased concentrations of importin-β, or of NUP-binding region, perturb this balance. To test this, we sought to restore the balance by coexpressing RANBP2 together with importin-β, then asked whether this would correct the defects caused by importin-β alone. We separately expressed three RANBP2 fragments (Joseph and Dasso, 2008): the encoded products are respectively devoid (BPN, RANBP2 N-terminal region 1–900) or rich (BPM, middle region 901–2219, and BPC, C-terminal region 2220–3224) in FG and FxFG repeats (Fig. S4 A). Regions in both BPM and BPC were previously shown to bind importin-β (Yaseen and Blobel, 1999). We established conditions in which RANBP2 fragments were expressed in a twofold excess over exogenous importin-β (Fig. 8 A; see Materials and methods). BPN associates with interphase MTs in hamster CHO cells (Joseph and Dasso, 2008), yet under our experimental conditions none of the RANBP2 derivatives, when expressed alone, altered the interphase cytoskeleton or mitotic progression in HeLa cells (Fig. S4, C and D). We then analyzed IF-stained mitoses from cultures cotransfected with importin-β and with single RANBP2 fragments. We found that the presence of either BPM or BPC constructs significantly reduced chromosome misalignment in metaphase and missegregation in anaphase and telophase compared with importin-β alone; the FG-devoid BPN construct was instead ineffective (Fig. 8, B and C). If overexpressed importin-β hinders RANGAP1 localization at KTs by interacting with RANBP2, then the exogenously expressed RANBP2 FG-rich fragment should compete with endogenous RANBP2 for importin-β and restore the endogenous RANBP2/SUMO–RANGAP1 complex availability. Indeed, cotransfection of BPM, but not BPN, with importin-β

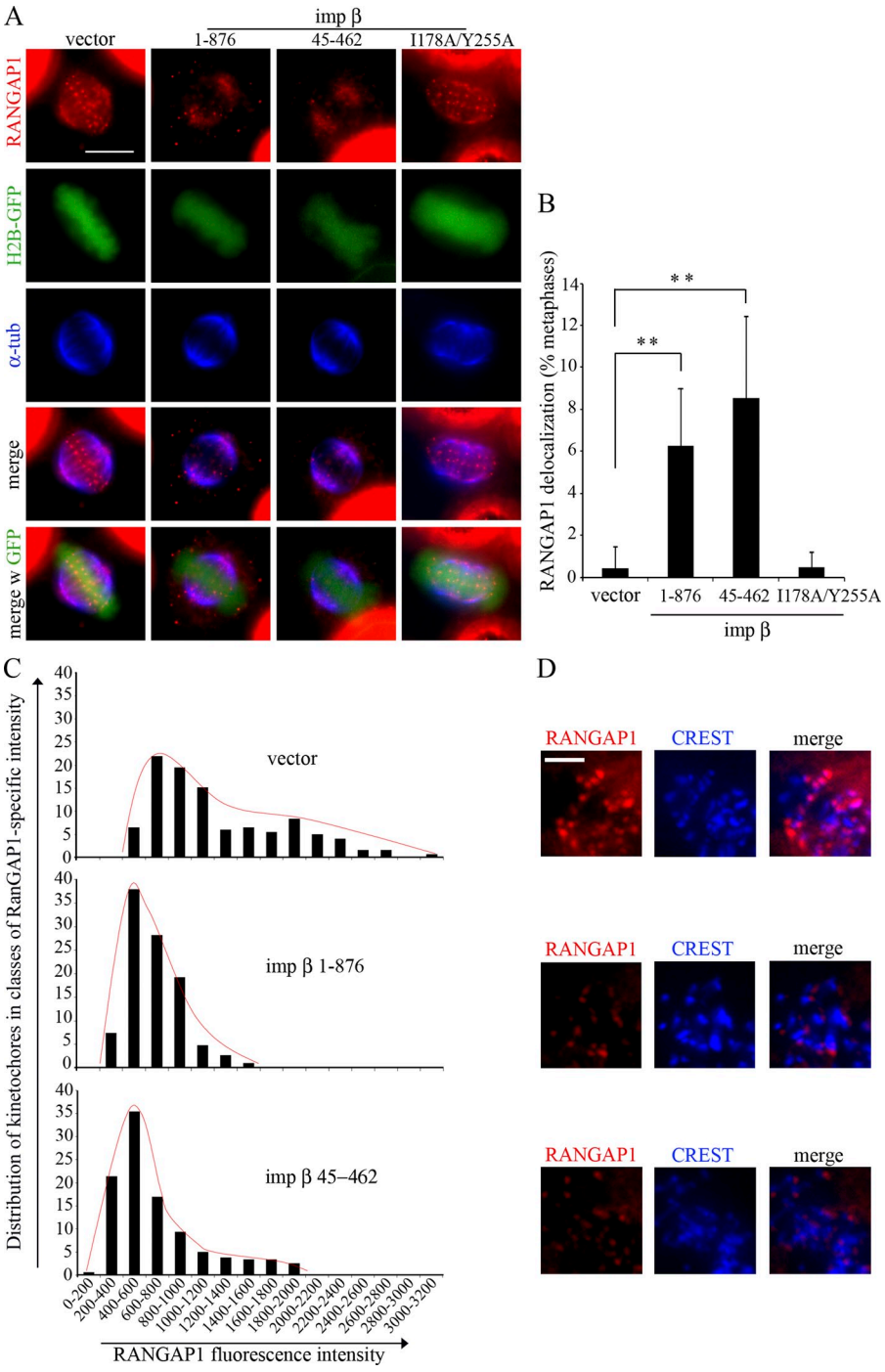

Figure 7. **Importin-β excess hinders RANGAP1 recruitment at KTs in metaphase cells.** (A) RANGAP1 localization in metaphase cells transfected with vector or with importin-β derivatives. H2B-GFP was cotransfected to visualize chromosomes. Bar, 10 µm. (B) Frequency of metaphase cells that lack RANGAP1 at KTs (320–450 scored metaphases per construct, 4 experiments). **, highly significant differences between cells transfected with importin-β 1–876 or 45–462 compared with controls ($P < 0.001$, $\chi 2$ test); there is no statistical difference between importin-β I178A/Y255A and controls. (C) Quantitative analysis of RANGAP1 recruitment to KTs in metaphase cells transfected with H2B-GFP and either importin-β 1–876, or 45–462, or vector. Transfected cells were identified for their green fluorescent chromosomes (not depicted), and RANGAP1-specific fluorescence signals were measured at single CREST-stained KTs. For each sample, the histograms represent the frequency (expressed as %) of KTs in the indicated classes of RANGAP1-specific fluorescence (*n*: 207 KTs in 6 independent counts for control samples, 236 KTs in 7 counts for importin-β–transfected samples, and 250 KTs in 8 counts for importin-β 45–462-transfected samples). KT-associated RANGAP1 signals range in classes of lower intensity values in importin-β 1–876- or 45–462-transfected cells compared with controls. (D) Examples of KTs in which RANGAP1-specific fluorescence was measured. Bar, 2 µm.

restored RANGAP1 localization to KTs in metaphase (Fig. 8 D). Finally, time-lapse assays revealed a significant decrease in mitotic dynamic defects, associated with significantly shorter prometaphase duration, in cotransfected cells compared with importin-β alone (Fig. 8 E).

Importin-β overexpression prevents RANGAP1 recruitment to KTs, yet does not mislocalize CRM1 off KTs (Fig. S2 A): thus, CRM1 remains competent to orchestrate RANGAP1 recruitment to KTs, but this function is overridden when importin-β is present in excess. This suggests that the balance between importin-β and CRM1 is critical to regulate the localization of RANBP2–RANGAP1 at KTs. We asked whether coexpressing CRM1 would oppose the inhibitory effect of importin-β alone. A typical CRM1–importin-β coexpression assay is shown in Fig. 8 A. Exogenous CRM1 localized correctly at the NE and in the nucleus in interphase (Fig. S5 D) and at MTs and KTs in mitosis (Fig. S5 E). Expression of CRM1 alone induced a mild yet constant increase in the frequency of misaligned metaphase chromosomes. Nevertheless, when coexpressed together with importin-β, CRM1 mitigated the mitotic abnormalities generated by importin-β alone: first, there was a significantly decreased induction of misaligned chromosomes in fixed cells processed for IF (Fig. 8 B, quantified in Fig. 8 C); second, the delay in prometaphase associated with abnormal

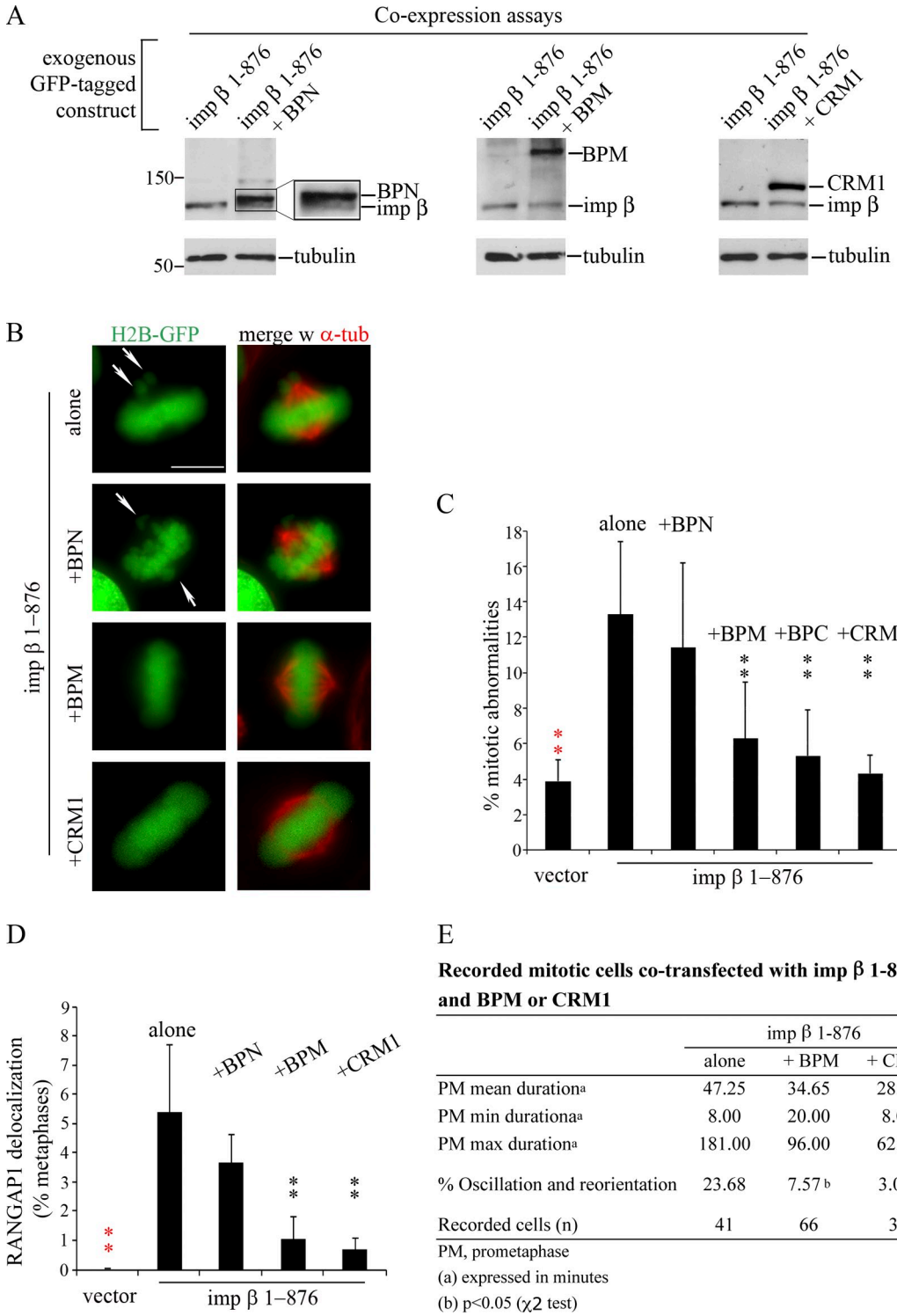

	imp β 1-876		
	alone	+ BPM	+ CRM1
PM mean duration[a]	47.25	34.65	28.55
PM min duration[a]	8.00	20.00	8.00
PM max duration[a]	181.00	96.00	62.00
% Oscillation and reorientation	23.68	7.57 [b]	3.03[b]
Recorded cells (n)	41	66	33

PM, prometaphase
(a) expressed in minutes
(b) $p<0.05$ ($\chi 2$ test)

Figure 8. **Co-expression of either RANBP2 or CRM1 reduces importin-β–dependent mitotic abnormalities.** (A) WB analysis of cell extracts transfected either with importin-β 1–876 (left lane in each panel) or with the indicated constructs (right lanes). Extracts were fractionated through 6% SDS-PAGE and constructs were detected using GFP antibody. (B) Mitotic cells transfected with importin-β 1–876 alone (top), or together with BPN, BPM, or CRM1. A trace of H2B-GFP was added to visualize chromosomes. Arrows point to chromosomes that fail to align. Z-stack (0.6–0.8 µm) images were flattened using the Maximum Intensity Projection tool (NIS-Elements 3.1; Nikon). Bar, 10 µm. (C) Frequency of mitotic defects in fixed cells transfected with importin-β alone or with RANBP2 fragments, or with CRM1 (740–2,000 counted cells per group, at least 5 experiments). **, highly significant ($P < 0.01$, χ^2 test) differences between importin-β and vector (in red), and between cotransfected samples compared with importin-β only (in black). No statistical difference was observed between importin-β alone and cotransfection with BPN. (D) Co-expression of either BPM or CRM1, but not BPN, rescues RANGAP1 localization to KTs. Histograms represent the frequency of metaphases with delocalized RANGAP1 from KTs (at least 350 counted cells per group, 4 experiments). **, highly significant ($P < 0.001$, χ^2 test) differences between importin-β and vector are indicated by red asterisks, and between cotransfected samples and importin-β alone by black asterisks. (E) Co-expression of either BPM or CRM1 reduces importin-β–dependent prometaphase delay and dynamic defects in video-recorded cells.

oscillations and unstable alignment was significantly reduced in time-lapse assays (Fig. 8 E). Finally, concomitant with this phenotypic correction, CRM1 restored RANGAP1 at KTs in importin-β–overexpressing cells (Fig. 8 D).

Discussion

Mitotic roles of importin-β mutants: The IAB in mitotic spindle pole organization

This work shows that importin-β regulates distinct aspects of mitosis through specific domains and interactions and pinpoints a novel role of importin-β in KT functions. By time-lapse imaging, importin-β overexpression disrupts several aspects of mitosis. Only a subset of defects, affecting the spindle bipolar organization, was previously identified in fixed cells (Nachury et al., 2001; Ciciarello et al., 2004; Kaláb et al., 2006). By recording cells undergoing their first mitosis after transfection of different importin-β mutants, we find that the induction of multipolar chromosome segregation depends on the integrity of the C-terminal region. This is consistent with previous findings that coexpressing TPX2 (which interacts with importin-α and, indirectly, with the importin-β IAB) mitigates the spindle pole defects (Ciciarello et al., 2004), confirming that importin-β negatively regulates NLS-containing spindle-organizing factors with which it interacts via the C-terminal region.

Importin-β regulates dynamic aspects of mitosis through NUP-binding sites

Unexpectedly, the spindle pole defects observed in fixed cells represent a minority of all importin-β–dependent mitotic abnormalities. The most frequently recorded abnormalities affect chromosome congression and alignment, stable positioning of the spindle axis, and SAC-dependent duration of prometaphase and metaphase. These abnormalities could not have been recognized in fixed cells, yet they have higher penetrance compared with structural defects, indicating a higher sensitivity to importin-β levels. These heterogeneous defects likely involve different downstream factors. A common feature is the implication of MT–plus end misfunction: chromosome misalignment and abnormal oscillations suggest unstable interactions of pole-originating MTs with KTs; the spindle rotations suggest defective interactions of astral MT–plus ends with the cell cortex. These abnormalities are induced particularly in cells expressing importin-β 45–462, which retains the ability to bind NUPs, e.g., RANBP2. In contrast, the NUP binding-defective importin-β I178A/Y255A, which generated spindle pole disruption, did not induce defects of the "dynamic" type. These mutants separate therefore distinct mitotic functions regulated by importin-β and assign a dominant-negative role to the 45–462 region in mitotic dynamic functions.

Importin-β interacts with RANBP2 and SUMO–RANGAP1 and negatively regulates RANGAP1 localization to mitotic KTs

Importin-β, RANBP2 and SUMO–RANGAP1 colocalize along the spindle (Joseph et al., 2002; Ciciarello et al., 2004) and all three interact in mitotic cells, therefore outside the context of structured NPCs. Polymerized MTs however are not necessary for their interaction, suggesting that, after NPC disassembly, they can interact even before the spindle is fully organized. MT attachment to KTs is a critical event, at which fractions of these components are targeted to distinct destinations: importin-β remains MT associated until anaphase, whereas part of RANBP2 and SUMO–RANGAP1 localize to KTs (Joseph et al., 2002, 2004).

It is unclear how exactly RANBP2/RANGAP1–SUMO are recruited to mitotic KTs, but it seems to involve a cascade of events. First, both CRM1 and RANGTP are required for recruitment (Arnaoutov et al., 2005), implicating a KT-based trimeric complex, similar to interphase export complexes. Second, RANGAP1 recruitment and/or stabilization at KTs requires Ska3/RAMA1, a protein involved in connecting KTs and MTs (Ohta et al., 2010), and the NUP107-160 complex, which localizes to KTs after NPC disassembly (Loïodice et al., 2004; Orjalo et al., 2006; Zuccolo et al., 2007) with potential roles in localizing Aurora-B and other passenger proteins (Platani et al., 2009). Third, the NUP107-160 complex is itself recruited to KTs in a manner dependent on Hec1 and Nuf2 (Zuccolo et al., 2007), both of which stabilize MT–KT attachments (Musacchio and Salmon, 2007). Thus, activities involved in RANGAP1 recruitment to KTs also regulate MT–KT attachments. Overexpression of importin-β, or of the 45–462 region, inhibits RANGAP1 localization at MT-attached KTs, whereas importin-β I178A/Y255A did not perturb it, clearly demonstrating that the inhibition is exerted via the NUP-binding domain.

Importin-β and CRM1 play opposing functions

We find that importin-β negatively regulates RANGAP1 at KTs in a manner dependent on RANBP2 binding. This function, detected here under conditions of overexpression as an experimental tool, is likely to operate physiologically from NPC disassembly to the completion of MT attachment. In early mitosis, RANGTP accumulation at KTs contributes to the spindle build-up: it regulates the nucleation of KT-originating fibers (Tulu et al., 2006; Torosantucci et al., 2008; Mishra et al., 2010); it facilitates KT "search-and-capture" by polar MTs (Wollman et al., 2005); furthermore, it regulates MT plus end–stabilizing factors (HURP, kid, and others) during KT attachment (Koffa et al., 2006; Silljé et al., 2006; Tahara et al., 2008). Concomitantly, the Aurora-B–MCAK system depolymerizes misattachments occurring as MTs establish random interactions with chromosomes. KTs are critical platforms over which these processes integrate and MT turnover at KTs is required at this stage. RANGAP1 recruitment to MT-attached KTs can provide a temporal device to activate RANGTP hydrolysis, so as to stop nucleation of KT-originated MTs, modulate MT turnover, and perhaps facilitate misattachment correction.

The data reported here suggest that importin-β prevents the dispersal of a functionally relevant fraction of RANBP2–RANGAP1 in the mitotic cytoplasm at NPC disassembly and helps their delivery to KTs upon MT attachment. Two independent "rescue" assays support this idea. First, we found that

coexpression of either of two FG-rich fragments from RANBP2, but not an FG-devoid region, together with importin-β, reduced dynamic mitotic abnormalities, restored prometaphase duration, and reestablished RANGAP1 onto MT-attached KTs. The RANBP2 fragments that proved effective have clearly distinct structural and functional features; their FG density and importin-β–binding ability (Yaseen and Blobel, 1999) is their only similarity. The rescuing ability of these otherwise different FG-rich RANBP2 fragments, and the ineffectiveness of the FG-devoid fragment, demonstrate the importance of the interaction between importin-β and RANBP2, or, in other words, of the balance between importin-β–bound and –free RANBP2/SUMO–RANGAP1.

Second, because MT attachment brings a RANBP2/SUMO–RANGAP1 fraction in close proximity of KTs, where CRM1 resides, we surmised that KT-associated CRM1 might exert an antagonistic function to that of importin-β in order to recruit the RANBP2/SUMO–RANGAP1 complex to KTs. Indeed, simultaneously raising the concentration of CRM1 and importin-β in coexpression assays restores RANGAP1 to MT-attached KTs and concomitantly reduces the induction of unstable chromosome alignment and mitotic delay. Thus, the balance of importin-β and CRM1 is critical to RANGAP1 mitotic localization. It is interesting to note that in some aggressively proliferating cancers, importin-β and CRM1 are simultaneously overexpressed (van der Watt et al., 2009).

Conclusions: Importin-β as a fine-tuner of mitosis in human cells

In conclusion, there is a continuity in the topological specificity of importin-β domains in interphase and in mitosis: domains that play spatially restricted functions in nuclear import (import complex assembly in the cytoplasm via the C-ter region, translocation through NPCs via NUP-binding sites, cargo release, and recycling out of the nucleus via the RAN-binding domain) distinctly regulate spindle pole formation, MT dynamic functions, and KT interactions in mitosis. Importin-β is not implicated in KT functions in XEEs and, in parallel, the RANGAP1–RANBP2 complex is undetectable at KTs in this system (Arnaoutov and Dasso, 2005). The contribution of importin-β to the regulation of RANGAP1 localization at attached KTs identifies therefore a specific pathway in mitotic somatic cells. In XEEs, MT nucleation and organization from chromatin requires a robust chromosome-centered RANGTP gradient acting as a positional signal (Caudron et al., 2005). In mammalian cells, the centrosome- and KT-driven spindle assembly pathways integrate (Maiato et al., 2004; O'Connell and Khodjakov, 2007), requiring spatially restricted, finely tuned signals. RANGTP and RANGAP1 localize in a mutually exclusive manner at KTs during KT-driven MT nucleation, associated with the recruitment of γ-tubulin complexes to KTs (Mishra et al., 2010), and relocalize when KT-dependent nucleation ceases (Torosantucci et al., 2008). The finding that importin-β contributes to the regulated delivery of RANGAP1 to MT-attached KTs advances our understanding of mitotic control operated by RAN effectors at specific mitotic structures in human cells.

Materials and methods

Cell culture and synchronization

Human HeLa epithelial cells (American Tissue Culture Collection, CCL-2) were grown in DME supplemented with 10% fetal calf serum (FCS), 2% L-glutamine, and 2% penicillin/streptomycin in a humidified atmosphere at 37°C in 5% CO_2. Where indicated, and particularly in time-lapse recoding experiments, cells were synchronized by culturing in 2 mM thymidine to arrest the cell cycle at the G1/S transition, then releasing in fresh medium containing 30 µM deoxycytidine to resume synchronous progression through S and G2 phases. To monitor cell cycle progression, cell samples were harvested at various times after the block release, stained with propidium iodide, and analyzed by FACS analysis in a Coulter Epics XL cytofluorimeter (Beckman Coulter). In some experiments, mitotic cells were isolated at round-up by shake-off 10 h after release from thymidine arrest, replated, and harvested at the indicated times. In some experiments cells were treated with 200 ng/ml nocodazole (Sigma-Aldrich) 8 h after release from thymidine arrest and harvested 6 h later.

Expression constructs and transfection experiments

The construct encoding full-length importin-β in the mammalian expression vector pEGFP-N1 (Takara Bio Inc.) was described previously (Ciciarello et al., 2004). The N-deleted (45–876), C-deleted (1–462) and N/C-deleted (45−462) versions were PCR amplified and cloned in pEGFP-N1 (Takara Bio Inc.). N-deleted (45–876) and C-deleted (1–462) inserts were also cloned in untagged pCMV vector. Importin-β I178A/Y255A was synthesized from the full-length construct using the QuikChange Lightning Multi Site-Directed Mutagenesis kit (Agilent Technologies) to replace codons ATC (position 534) and TAT (position 765) with GCC and GCT, respectively. The mutant sequence was verified using the BigDye Terminator v1.1 Cycle Sequencing system (Applied Biosystems) in a 48-capillary 3730 DNA Analyzer (Applied Biosystems). Both the mutagenesis and sequencing services were provided by Bio-Fab Research at Sapienza University (Rome, Italy). All other mammalian gene sequences used in this work are also expressed under the CMV promoter from similar expression vectors. The pRCC1 construct was described previously (De Luca et al., 2003) and contains the human RCC1 coding region cloned in frame with an HA tag in pBluescript. Constructs BPN, BPM, and BPC were a kind gift from Jomon Joseph (National Centre for Cell Science, Ganeshkhind, Pune, India) and they correspond respectively to RANBP2 regions 1–900 (N-terminal fragment), 901–2219 (middle fragment), and 2220–3224 cloned into pEGFP-C vectors (Joseph and Dasso, 2008). The CRM1-GFP construct, kindly provided by Marteen Fornerod (Erasmus University Medical Center, Rotterdam, Netherlands), contains the entire CRM1 open reading frame cloned in frame with GFP in the pCDNA3 vector. In experiments with untagged constructs and in time-lapse recording assays, a trace of H2B-GFP plasmid (containing the H2B coding sequence cloned into pEGFP-N1) was included in the transfection mix to visualize chromosomes. All controls were transfected with pEGFP or with a mixture of pCMV and H2B-GFP plasmids. The pSUPER-Mad2 construct (a kind gift from Anna De Antoni and Andrea Musacchio, European Institute of Oncology, Milan, Italy) harbors a short hairpin RNA (shRNA)–encoding fragment targeting the *Mad2* gene sequence 5′-GGAAGAGTCGGGACCACCACAG-3′. pSUPER devoid of shRNAs was used for control. Plasmids were transfected using Lipofectamine 2000 (0.8–1 µl/µg DNA; Invitrogen) or Metafectene Easy (1 µl/µg DNA; Biontex).

Earlier transfection experiments with importin-β (Ciciarello et al., 2004) had shown that importin-β plasmid doses >2.5 µg per 10^6 HeLa cells reduce the mitotic index, paralleled by an increase in interphase cells expressing cyclin B1 (therefore in G2) in transfected compared with control cultures, presumably reflecting a severe inhibitory effect on mitotic MT formation. Nuclear transport was functional, however, as judged by proper cyclin B1 localization in nuclei. We used plasmid concentrations <2.5 µg per 10^6 HeLa cells for importin-β constructs 1–876, 45–876, and I178A/Y255A, and 2.0 µg per 10^6 HeLa cells for constructs 1–462 and 45–462. To quantify exogenous proteins, transfected cultures were grown in culture dishes containing a sterile coverslip. The transfection rate was calculated after staining the cells on the coverslip with DAPI and counting GFP-positive cells/DAPI-stained nuclei: routinely, plasmid doses used in this study yield 30–40% transfected cells. Protein extracts prepared from the rest of the culture were fractionated through SDS-PAGE and analyzed by WB. Exogenous importin-β signals were measured and corrected for the transfection rate: in different experiments, exogenous importin-β (wild-type or derivatives) has a 1.5- to 2.0-fold abundance relative to the endogenous (taken as 1; Fig. S1 B), yielding a corresponding 2.5- to 3.0-fold increase in the overall importin-β concentration in transfected cells (average values).

Variations in the abundance of exogenous importin-β (or derivative constructs) were measured quantitatively at the single-cell level: cultures transfected with GFP-tagged importin-β constructs, or with pEGFP for control, were processed using importin-β antibody and secondary red-emitting antibody; images were taken under identical acquisition parameters and red-emitting signals were quantified in GFP-positive cells. The distribution of single transfected cells in classes of importin-β fluorescence-specific intensity is shown in Fig. S1 D.

Cotransfection mixes were set using 2.5:1 ratios of "rescuing" plasmid (encoding RANBP2 fragments or CRM1) to importin-β (all GFP-tagged; the ratios were calculated taking into account the size of the open reading frames under analysis). WB were analyzed using (i) GFP antibody, to verify the relative intensity of exogenously expressed rescuing protein and importin-β 1–876, all GFP tagged (Fig. 8); this indicated that RANBP2-derived and CRM1 products are ∼2- to 2.5-fold more abundant than cotransfected importin-β, and (ii) domain-specific antibodies for both RANBP2 (Fig. S4 B) and CRM1 (Fig. S5 A), correcting the exogenous signal intensity for the transfection rate as above, to calculate overexpression: RANBP2-derived fragments are ∼2- to 2.5-fold more abundant than the endogenous RANBP2, and exogenous CRM1 expression increased the overall intracellular abundance of CRM1 by about threefold. IF measurements were not reliable for RANBP2 fragments, given the different size and different reactivity of exogenous compared with endogenous RANBP2. Quantitative IF for CRM1 was performed as described above, using antibodies that recognize preferentially either the NE- and KT-associated, or the nuclear fraction, consistently indicating a two- to threefold increase in CRM1 abundance in transfected cells compared with controls (Fig. S5, B and C).

Immunofluorescence and microscopy

Cells grown on sterile glass coverslips were fixed following one of the following protocols: (i) direct fixation in 3.7% paraformaldehyde (PFA)/30 mM sucrose (to visualize the entire pool of the protein under examination at their intracellular sites); (ii) simultaneous solubilization/fixation in 100% methanol; (iii) preincubation in 0.1% Triton X-100 in PHEM (45 mM Hepes, pH 6.9, 45 mM Pipes, pH 6.9, 10 mM EGTA, 5 mM $MgCl_2$, and 1 mM PMSF) before fixing in 3.7% PFA/30 mM sucrose, to remove soluble proteins and visualize their association with mitotic structures; or (iv) preextraction in 0.005% digitonin in transport buffer (110 mM KOAc, 2 mM $Mg(OAc)_2$, 0.5 mM EGTA, and 20 mM Hepes) before fixation, to obtain high resolution images of KT-associated proteins. The latter procedure solubilizes much of the exogenously expressed importin-β–derived proteins; H2B-GFP was therefore included in the transfection mix to identify transfected cells, as histone incorporation in chromatin resists solubilization protocols.

Primary antibodies included: α-tubulin, either unconjugated (B5-1-2) or FITC-conjugated (DM1A), both from Sigma-Aldrich; RANGAP1 (H-180, raised against region 408–587, and N-19, recognizing the N terminus; both from Santa Cruz Biotechnology, Inc.); CREST (15–234-0001, Antibodies Inc.); CENP-F (NB500-101; Novus Biologicals); BUB1 (MAB3610; Millipore); importin-β (ab2811, Abcam; or clone 23; BD); CRM1 (611833 raised against region 2–122, BD; and H-300 raised against region 772–1071, Santa Cruz Biotechnology, Inc.); TPX2 antibody was either from Novus Biologicals (NB500-179), or was made in-house at EMBL (Heidelberg, Germany) and kindly given by Dr. Iain Mattaj. Secondary antibodies were conjugated to FITC, Cy3, or 7-amino-4-methylcoumarin-3-acetic acid (AMCA; Jackson Immunoresearch Laboratories, Inc.), rhodamine (Santa Cruz Biotechnology, Inc.), or Texas red (Vector Laboratories). DNA was stained with 0.1 µg/ml DAPI and coverslips were mounted in Vectashield (Vector Laboratories).

Cells were examined under epifluorescence microscopes, using either an Olympus Vanox equipped with a SPOT CCD camera (Diagnostic Instruments), acquiring color encoded images using ISO 2000 software (Delta Sistemi) or using a Nikon Eclipse 90i with a Qicam Fast 1394 camera and acquiring images with NIS-Elements AR 3.1 (Nikon). Single-cell images were routinely taken using immersion oil 100x objectives with NA 1.3 (90i; Nikon) or NA 1.35 (Olympus). Where indicated, a 40x objective with NA 0.75 was used to acquire entire fields. All images were processed with Photoshop CS 8.0. Three dimensional (3D) deconvolution and reconstruction of images taken under the Olympus Vanox microscope were processed through 0.3-µm z-serial optical sections using the AutoDeblur 9.3 (AutoQuant Imaging, Inc.) image processing program. For quantitative immunofluorescence of RANGAP1 signals at single KTs, z-stacks (0.6 µm distance) were taken under a Nikon Eclipse 90i, then deconvolved using the NIS-Elements AR 3.1 algorithms and flattened using the Maximum Intensity Projection tool to quantify RANGAP1-specific fluorescence signals associated with KTs.

Time-lapse imaging

Cells to be video recorded were seeded in glass-bottomed 3.5-cm^2 plates (81156, IbiTreat; Ibidi) and transfected with relevant constructs on the following day. 6 h after transfection, the medium was changed and cultures were synchronized by thymidine block/release as described previously (Tedeschi et al., 2007). Just before recording, the medium was changed to red phenol-free Leibovitz's L-15 medium supplemented with 1% nonessential amino acids and 20 mM Hepes. During recording, cell cultures were kept at 37°C in a temperature- and CO_2-controlled microscope stage incubator (Basic WJ; Okolab). Cultures were either recorded under an inverted microscope (Eclipse TE300; Nikon) equipped with a digital camera (1280 × 1024 pixel resolution; DXM 1200, Nikon) and the ACT-1 software, or under an automated inverted microscope (Ti Eclipse; Nikon) equipped with a DS-Qi1MC camera, an Intensilight C-HGFIE lamp, and the NIS-Elements 3.1 software (all from Nikon). Phase-contrast (60x, 0.7 NA) or immersion oil (60x, 1.4 NA) objectives were used. Mitotic cells were recorded for 6–24 h. Bright-field images (phase-contrast or differential interference contrast) were taken every 2–3 min and GFP-fluorescence images every 20–30 min

Western immunoblotting

Whole-cell extracts (WCE) were prepared from cell cycle–staged HeLa cell populations, separated through SDS-PAGE, transferred to nitrocellulose filters, blocked, and incubated with antibodies as described previously (Ciciarello et al., 2010). WCE to be used in IP assays were routinely prepared in 1D buffer (1% NP-40, 50 mM Tris-HCl, pH 8.0, 150 mM NaCl, 1 mM EGTA, and 1 mM EDTA) or in RIPA (1D buffer supplemented with 0.1% SDS, 0.25% sodium deoxycholate, and 50 mM *N*-ethylmaleimide) to compare SUMO-conjugated RANGAP1 forms. Protein extracts were routinely separated through 6–12% SDS-PAGE, yet particular conditions were used to visualize specific proteins: for RANBP2, 6% (1:29 bis/acrylamide ratio); for modified RANGAP1 forms, either 6% (1:29 bis/acrylamide) or 8% (1:50 bis/acrylamide); for importin-β mutant forms, 9 or 10% (1:60 or 1:76 bis/acrylamide, respectively). Molecular weight markers were either the prestained BenchMark protein markers (Invitrogen) or Precision Plus or Broad Range protein standards (both from Bio-Rad Laboratories).

Commercial primary antibodies were as follows: to actin (I-19), RANGAP1 (N-19 or H-180), RANBP2 (N-20, binding the N-terminal fragment), and RAN (C-20), from Santa Cruz Biotechnology, Inc.; to importin-β/karyopherin-β (clone 23) and CRM1 (clone 17), from BD; to RANBP2 (ab64276, raised against a repeated peptide at positions 1592–1607, 1651–1666, and 1710–1725 in the human RANBP2 protein) and importin-β (ab2811), from Abcam; and to GFP (11814460001) from Roche. Antibody to Mad2 was a kind gift from Dr. Andrea Musacchio (European Institute of Oncology, Milan, Italy). HRP-conjugated secondary antibodies (Santa Cruz Biotechnology, Inc.) were revealed using ECL or ECL plus (GE Healthcare). ECL signals were either revealed on Hyperfilm-ECL films (GE Healthcare) or were detected using Image Station 440cf (Kodak) and quantified using either ImageJ (National Institutes of Health, Bethesda, MD) or Photoshop CS 8.0.

Co-IP assays

HeLa cells were lysed in 1D buffer containing protease and phosphatase inhibitors (aprotinin, leupeptin, and pepstatin, all 1 µg/ml; 1 mM PMSF, 50 mM NaF, and 2 mM Na_3VO_4). Lysates were precleared with Protein G–Sepharose 4 Fast Flow (GE Healthcare) at 4°C for 1 h. The precleared supernatant was incubated with one of the following antibodies: (i) anti–importin-β antibody (ab2811, Abcam; and I2534, Sigma-Aldrich were compared, yielding comparable patterns); (ii) anti-RANBP2 (N-20; Santa Cruz Biotechnology, Inc.); (iii) anti-GFP (11814460001, Roche) for exogenously expressed constructs; or (iv) anti–mouse (Cappel) or anti–rabbit (sc-2091; Santa Cruz Biotechnology) IgG for control. The antibody/lysate complexes were incubated on a stirring wheel at 4°C overnight, then mixed with beads for 3 h at 4°C. At the end of incubation the resin was washed 5x in 1D buffer and protein complexes were eluted 3x in loading buffer (50 mM Tris-HCl, pH 6.8, 2% SDS, 10% glycerol, and 100 mM DTT), heated at 95°C for 5 min and centrifuged for 5 min at 3,000 rpm at 4°C to sediment the beads. Proteins in the supernatant were separated through SDS-PAGE and analyzed by WB.

In-gel digestion, mass spectrometry analysis, and database search

Co-IPed proteins were separated through SDS-PAGE and stained with Coomassie blue. Visible bands were manually excised from the gel, cut into small pieces of ∼1 mm^3, and submitted to in-gel digestion using sequencing grade trypsin (Promega) as described elsewhere (Shevchenko et al., 2006). The excised gel pieces were washed in 50 mM ammonium bicarbonate in 50% (vol/vol) acetonitrile, dehydrated in 100% acetonitrile, and dried in a vacuum concentrator. Samples were reduced with 10 mM DTT in 50 mM ammonium bicarbonate and subsequently alkylated by incubation with

55 mM iodoacetamide in 50 mM ammonium bicarbonate. Gel bands were washed, dehydrated, and speed-vac dried. Gel pieces were then rehydrated by adding 25 mM ammonium bicarbonate containing 11 ng/µl trypsin and incubated on ice. After 30 min, trypsin buffer was added and gel pieces were incubated at 37°C for 16 h. Digested aliquots were analyzed either directly or after a desalting/concentration step on µZipTipC18 according to the manufacturer's instructions (Millipore). 1 µl of the supernatant from the digestion was mixed (1:1 vol/vol) with saturated matrix solution (α-cyano-4-hydroxycinnamic acid in 70% acetonitrile/0.1% TFA or dihydroxybenzoic acid in 50% acetonitrile/0.1% TFA) and loaded onto the MALDI target using the dried droplet technique. MALDI-MS measurements were performed on a Voyager-DE STR time-of-flight (TOF) mass spectrometer (Applied Biosystems) operating in positive ion reflectron mode. All mass spectra were externally calibrated using a standard peptide mixture containing des-Arg-bradykinin (*m/z* 904.4681), angiotensin I (*m/z* 1296.6853), 1–17 (*m/z* 2093.0867), and 18–39 (*m/z* 2465.1989) adrenocorticotropic hormone fragments. Spectra were collected over the mass range of 800–5,000 D and processed via the MoverZ software (Proteometrics LLC) according to default parameters. Two monoisotopic peaks from a known auto-digestion product of bovine trypsin were also used for the internal calibration (*m/z* 842.5100 and 2807.3145). Proteins were identified by matching monoisotopic peptide mass lists against the SwissProt Homo sapiens database (v. 2010_10, 521016 sequences, 183900292 residues; and v. 56.7, 408099 sequences, 147085246 residues) using Mascot Search engine. Known keratin masses and trypsin autodigest products were excluded using the PeakErazor software. Matching parameters generally selected in the search program were: maximum error of 50 ppm, until one missed trypsin cleavage, oxidation of methionine residues as dynamic modification, and carbamidomethylated cysteine residues as fixed modification. The sequence coverage percentage for each band is reported in Table S1. Identifications were validated when the probability-based Mowse protein score was significant according to Mascot. Only proteins with Mowse scores >56 were considered significantly matched ($P < 0.05$).

Online supplemental material

Fig. S1 shows the maps of importin-β mutant constructs as well as their expression in HeLa cells, detected by coupled WB assays of transfected HeLa cells at the cell population level and by IF to assess variations at the single cell-level. Fig. S2 shows that importin-β overexpression alters the KT localization at CENP-F but not that of CRM1. Fig. S3 shows that importin-β overexpression neither affects BUB1 signals on misaligned kinetochores nor their disappearance in anaphase. Fig. S4 shows that, at the concentrations used in this study, transfected RANBP2-derived fragments neither induce mitotic abnormalities nor do they alter the cytoskeleton organization. Fig. S5 shows that exogenously expressed CRM1-GFP localizes correctly in the nucleus and at the nuclear rim of interphase cells and at KTs of mitotic cells like the endogenous protein. Video 1 shows normal mitosis in a vector/H2B-GFP-transfected HeLa cell (still frames in Fig. 1 A). Video 2 shows a multipolar division of a HeLa cell transfected with importin-β and H2B-GFP (still frames in Fig. 1 B). Video 3 shows repeated cycles of chromosome alignment and redispersal, with an abnormal prometaphase duration, in a HeLa cell transfected with importin-β and H2B-GFP (still frames in Fig. 1 C). Video 4 shows spindle axis rotation during an abnormally prolonged metaphase in a HeLa cell transfected with importin-β and H2B-GFP (still frames in Fig. 1 D). Table S1 shows the details of protein identification after peptide mass fingerprinting, using the Mascot search engine, for RANBP2, importin-β, RANGAP1, and SUMO-1, RANBP1, and RAN. Online supplemental material is available at http://www.jcb.org/cgi/content/full/jcb.201109104/DC1.

We are grateful to Aktan Alpsoy, Ann-Christine Bauke, Alessandra Giorgi, and Alessandra Ruggiero for contributions and to Giulia Guarguaglini and the Nikon Italia team for advice and assistance with time-lapse imaging.

This work was supported by the Italian Association for Cancer Research (AIRC, IG10164), PRIN (200879X9N9-004), and Fondazione Monte dei Paschi di Siena.

Submitted: 21 September 2011
Accepted: 18 January 2012

References

Arnaoutov, A., and M. Dasso. 2003. The Ran GTPase regulates kinetochore function. *Dev. Cell*. 5:99–111. http://dx.doi.org/10.1016/S1534-5807(03)00194-1

Arnaoutov, A., and M. Dasso. 2005. Ran-GTP regulates kinetochore attachment in somatic cells. *Cell Cycle*. 4:1161–1165. http://dx.doi.org/10.4161/cc.4.9.1979

Arnaoutov, A., Y. Azuma, K. Ribbeck, J. Joseph, Y. Boyarchuk, T. Karpova, J. McNally, and M. Dasso. 2005. Crm1 is a mitotic effector of Ran-GTP in somatic cells. *Nat. Cell Biol.* 7:626–632. http://dx.doi.org/10.1038/ncb1263

Bayliss, R., T. Littlewood, and M. Stewart. 2000. Structural basis for the interaction between FxFG nucleoporin repeats and importin-beta in nuclear trafficking. *Cell*. 102:99–108. http://dx.doi.org/10.1016/S0092-8674(00)00014-3

Bayliss, R., T. Littlewood, L.A. Strawn, S.R. Wente, and M. Stewart. 2002. GLFG and FxFG nucleoporins bind to overlapping sites on importin-beta. *J. Biol. Chem.* 277:50597–50606. http://dx.doi.org/10.1074/jbc.M209037200

Bednenko, J., G. Cingolani, and L. Gerace. 2003. Importin beta contains a COOH-terminal nucleoporin binding region important for nuclear transport. *J. Cell Biol.* 162:391–401. http://dx.doi.org/10.1083/jcb.200303085

Ben-Efraim, I., and L. Gerace. 2001. Gradient of increasing affinity of importin beta for nucleoporins along the pathway of nuclear import. *J. Cell Biol.* 152:411–417. http://dx.doi.org/10.1083/jcb.152.2.411

Caudron, M., G. Bunt, P. Bastiaens, and E. Karsenti. 2005. Spatial coordination of spindle assembly by chromosome-mediated signaling gradients. *Science*. 309:1373–1376. http://dx.doi.org/10.1126/science.1115964

Chen, T., T.L. Muratore, C.E. Schaner-Tooley, J. Shabanowitz, D.F. Hunt, and I.G. Macara. 2007. N-terminal alpha-methylation of RCC1 is necessary for stable chromatin association and normal mitosis. *Nat. Cell Biol.* 9:596–603. http://dx.doi.org/10.1038/ncb1572

Ciciarello, M., R. Mangiacasale, C. Thibier, G. Guarguaglini, E. Marchetti, B. Di Fiore, and P. Lavia. 2004. Importin beta is transported to spindle poles during mitosis and regulates Ran-dependent spindle assembly factors in mammalian cells. *J. Cell Sci.* 117:6511–6522. http://dx.doi.org/10.1242/jcs.01569

Ciciarello, M., R. Mangiacasale, and P. Lavia. 2007. Spatial control of mitosis by the GTPase Ran. *Cell. Mol. Life Sci.* 64:1891–1914. http://dx.doi.org/10.1007/s00018-007-6568-2

Ciciarello, M., E. Roscioli, B. Di Fiore, L. Di Francesco, F. Sobrero, D. Bernard, R. Mangiacasale, A. Harel, M.E. Schininà, and P. Lavia. 2010. Nuclear reformation after mitosis requires downregulation of the Ran GTPase effector RanBP1 in mammalian cells. *Chromosoma*. 119:651–668. http://dx.doi.org/10.1007/s00412-010-0286-5

Cingolani, G., C. Petosa, K. Weis, and C.W. Müller. 1999. Structure of importin-beta bound to the IBB domain of importin-alpha. *Nature*. 399:221–229. http://dx.doi.org/10.1038/20367

Clarke, P.R., and C. Zhang. 2008. Spatial and temporal coordination of mitosis by Ran GTPase. *Nat. Rev. Mol. Cell Biol.* 9:464–477. http://dx.doi.org/10.1038/nrm2410

Dasso, M. 2006. Ran at kinetochores. *Biochem. Soc. Trans.* 34:711–715. http://dx.doi.org/10.1042/BST0340711

Dawlaty, M.M., L. Malureanu, K.B. Jeganathan, E. Kao, C. Sustmann, S. Tahk, K. Shuai, R. Grosschedl, and J.M. van Deursen. 2008. Resolution of sister centromeres requires RanBP2-mediated SUMOylation of topoisomerase IIalpha. *Cell*. 133:103–115. http://dx.doi.org/10.1016/j.cell.2008.01.045

De Luca, A., R. Mangiacasale, A. Severino, L. Malquori, A. Baldi, A. Palena, A.M. Mileo, P. Lavia, and M.G. Paggi. 2003. E1A deregulates the centrosome cycle in a Ran GTPase-dependent manner. *Cancer Res.* 63:1430–1437.

Gruss, O.J., and I. Vernos. 2004. The mechanism of spindle assembly: functions of Ran and its target TPX2. *J. Cell Biol.* 166:949–955. http://dx.doi.org/10.1083/jcb.200312112

Gruss, O.J., R.E. Carazo-Salas, C.A. Schatz, G. Guarguaglini, J. Kast, M. Wilm, N. Le Bot, I. Vernos, E. Karsenti, and I.W. Mattaj. 2001. Ran induces spindle assembly by reversing the inhibitory effect of importin alpha on TPX2 activity. *Cell*. 104:83–93. http://dx.doi.org/10.1016/S0092-8674(01)00193-3

Hamada, M., A. Haeger, K.B. Jeganathan, J.H. van Ree, L. Malureanu, S. Wälde, J. Joseph, R.H. Kehlenbach, and J.M. van Deursen. 2011. Ran-dependent docking of importin-beta to RanBP2/Nup358 filaments is essential for protein import and cell viability. *J. Cell Biol.* 194:597–612. http://dx.doi.org/10.1083/jcb.201102018

Harel, A., and D.J. Forbes. 2004. Importin beta: conducting a much larger cellular symphony. *Mol. Cell*. 16:319–330.

Hughes, J.R., A.M. Meireles, K.H. Fisher, A. Garcia, P.R. Antrobus, A. Wainman, N. Zitzmann, C. Deane, H. Ohkura, and J.G. Wakefield. 2008. A microtubule interactome: complexes with roles in cell cycle and mitosis. *PLoS Biol.* 6:e98. http://dx.doi.org/10.1371/journal.pbio.0060098

Joseph, J., and M. Dasso. 2008. The nucleoporin Nup358 associates with and regulates interphase microtubules. *FEBS Lett.* 582:190–196. http://dx.doi.org/10.1016/j.febslet.2007.11.087

Joseph, J., S.H. Tan, T.S. Karpova, J.G. McNally, and M. Dasso. 2002. SUMO-1 targets RanGAP1 to kinetochores and mitotic spindles. *J. Cell Biol.* 156:595–602. http://dx.doi.org/10.1083/jcb.200110109

Joseph, J., S.T. Liu, S.A. Jablonski, T.J. Yen, and M. Dasso. 2004. The RanGAP1-RanBP2 complex is essential for microtubule-kinetochore interactions in vivo. *Curr. Biol.* 14:611–617. http://dx.doi.org/10.1016/j.cub.2004.03.031

Kalab, P., and R. Heald. 2008. The RanGTP gradient - a GPS for the mitotic spindle. *J. Cell Sci.* 121:1577–1586. http://dx.doi.org/10.1242/jcs.005959

Kaláb, P., A. Pralle, E.Y. Isacoff, R. Heald, and K. Weis. 2006. Analysis of a RanGTP-regulated gradient in mitotic somatic cells. *Nature*. 440:697–701. http://dx.doi.org/10.1038/nature04589

Klein, U.R., M. Haindl, E.A. Nigg, and S. Muller. 2009. RanBP2 and SENP3 function in a mitotic SUMO2/3 conjugation-deconjugation cycle on Borealin. *Mol. Biol. Cell*. 20:410–418. http://dx.doi.org/10.1091/mbc.E08-05-0511

Koffa, M.D., C.M. Casanova, R. Santarella, T. Köcher, M. Wilm, and I.W. Mattaj. 2006. HURP is part of a Ran-dependent complex involved in spindle formation. *Curr. Biol.* 16:743–754. http://dx.doi.org/10.1016/j.cub.2006.03.056

Kutay, U., E. Izaurralde, F.R. Bischoff, I.W. Mattaj, and D. Görlich. 1997. Dominant-negative mutants of importin-beta block multiple pathways of import and export through the nuclear pore complex. *EMBO J.* 16:1153–1163. http://dx.doi.org/10.1093/emboj/16.6.1153

Loïodice, I., A. Alves, G. Rabut, M. Van Overbeek, J. Ellenberg, J.B. Sibarita, and V. Doye. 2004. The entire Nup107-160 complex, including three new members, is targeted as one entity to kinetochores in mitosis. *Mol. Biol. Cell*. 15:3333–3344. http://dx.doi.org/10.1091/mbc.E03-12-0878

Mahajan, R., L. Gerace, and F. Melchior. 1998. Molecular characterization of the SUMO-1 modification of RanGAP1 and its role in nuclear envelope association. *J. Cell Biol.* 140:259–270. http://dx.doi.org/10.1083/jcb.140.2.259

Maiato, H., C.L. Rieder, and A. Khodjakov. 2004. Kinetochore-driven formation of kinetochore fibers contributes to spindle assembly during animal mitosis. *J. Cell Biol.* 167:831–840. http://dx.doi.org/10.1083/jcb.200407090

Matunis, M.J., J. Wu, and G. Blobel. 1998. SUMO-1 modification and its role in targeting the Ran GTPase-activating protein, RanGAP1, to the nuclear pore complex. *J. Cell Biol.* 140:499–509. http://dx.doi.org/10.1083/jcb.140.3.499

Mishra, R.K., P. Chakraborty, A. Arnaoutov, B.M. Fontoura, and M. Dasso. 2010. The Nup107-160 complex and gamma-TuRC regulate microtubule polymerization at kinetochores. *Nat. Cell Biol.* 12:164–169. http://dx.doi.org/10.1038/ncb2016

Moore, W., C. Zhang, and P.R. Clarke. 2002. Targeting of RCC1 to chromosomes is required for proper mitotic spindle assembly in human cells. *Curr. Biol.* 12:1442–1447. http://dx.doi.org/10.1016/S0960-9822(02)01076-X

Mosammaparast, N., and L.F. Pemberton. 2004. Karyopherins: from nuclear-transport mediators to nuclear-function regulators. *Trends Cell Biol.* 14:547–556. http://dx.doi.org/10.1016/j.tcb.2004.09.004

Musacchio, A., and E.D. Salmon. 2007. The spindle-assembly checkpoint in space and time. *Nat. Rev. Mol. Cell Biol.* 8:379–393. http://dx.doi.org/10.1038/nrm2163

Nachury, M.V., T.J. Maresca, W.C. Salmon, C.M. Waterman-Storer, R. Heald, and K. Weis. 2001. Importin beta is a mitotic target of the small GTPase Ran in spindle assembly. *Cell*. 104:95–106. http://dx.doi.org/10.1016/S0092-8674(01)00194-5

O'Connell, C.B., and A.L. Khodjakov. 2007. Cooperative mechanisms of mitotic spindle formation. *J. Cell Sci.* 120:1717–1722. http://dx.doi.org/10.1242/jcs.03442

Ohta, S., J.C. Bukowski-Wills, L. Sanchez-Pulido, Fde.L. Alves, L. Wood, Z.A. Chen, M. Platani, L. Fischer, D.F. Hudson, C.P. Ponting, et al. 2010. The protein composition of mitotic chromosomes determined using multiclassifier combinatorial proteomics. *Cell*. 142:810–821. http://dx.doi.org/10.1016/j.cell.2010.07.047

Orjalo, A.V., A. Arnaoutov, Z. Shen, Y. Boyarchuk, S.G. Zeitlin, B. Fontoura, S. Briggs, M. Dasso, and D.J. Forbes. 2006. The Nup107-160 nucleoporin complex is required for correct bipolar spindle assembly. *Mol. Biol. Cell*. 17:3806–3818. http://dx.doi.org/10.1091/mbc.E05-11-1061

Pichler, A., A. Gast, J.S. Seeler, A. Dejean, and F. Melchior. 2002. The nucleoporin RanBP2 has SUMO1 E3 ligase activity. *Cell*. 108:109–120. http://dx.doi.org/10.1016/S0092-8674(01)00633-X

Platani, M., R. Santarella-Mellwig, M. Posch, R. Walczak, J.R. Swedlow, and I.W. Mattaj. 2009. The Nup107-160 nucleoporin complex promotes mitotic events via control of the localization state of the chromosome passenger complex. *Mol. Biol. Cell*. 20:5260–5275. http://dx.doi.org/10.1091/mbc.E09-05-0377

Roscioli, E., A. Bolognesi, G. Guarguaglini, and P. Lavia. 2010. Ran control of mitosis in human cells: gradients and local signals. *Biochem. Soc. Trans.* 38:1709–1714. http://dx.doi.org/10.1042/BST0381709

Salina, D., P. Enarson, J.B. Rattner, and B. Burke. 2003. Nup358 integrates nuclear envelope breakdown with kinetochore assembly. *J. Cell Biol.* 162:991–1001. http://dx.doi.org/10.1083/jcb.200304080

Shevchenko, A., H. Tomas, J. Havlis, J.V. Olsen, and M. Mann. 2006. In-gel digestion for mass spectrometric characterization of proteins and proteomes. *Nat. Protoc.* 1:2856–2860. http://dx.doi.org/10.1038/nprot.2006.468

Silljé, H.H., S. Nagel, R. Körner, and E.A. Nigg. 2006. HURP is a Ran-importin beta-regulated protein that stabilizes kinetochore microtubules in the vicinity of chromosomes. *Curr. Biol.* 16:731–742. http://dx.doi.org/10.1016/j.cub.2006.02.070

Ström, A.C., and K. Weis. 2001. Importin-beta-like nuclear transport receptors. *Genome Biol.* 2:S3008. http://dx.doi.org/10.1186/gb-2001-2-6-reviews3008

Swaminathan, S., F. Kiendl, R. Körner, R. Lupetti, L. Hengst, and F. Melchior. 2004. RanGAP1*SUMO1 is phosphorylated at the onset of mitosis and remains associated with RanBP2 upon NPC disassembly. *J. Cell Biol.* 164:965–971. http://dx.doi.org/10.1083/jcb.200309126

Tahara, K., M. Takagi, M. Ohsugi, T. Sone, F. Nishiumi, K. Maeshima, Y. Horiuchi, N. Tokai-Nishizumi, F. Imamoto, T. Yamamoto, et al. 2008. Importin-beta and the small guanosine triphosphatase Ran mediate chromosome loading of the human chromokinesin Kid. *J. Cell Biol.* 180:493–506. http://dx.doi.org/10.1083/jcb.200708003

Tedeschi, A., M. Ciciarello, R. Mangiacasale, E. Roscioli, W.M. Rensen, and P. Lavia. 2007. RANBP1 localizes a subset of mitotic regulatory factors on spindle microtubules and regulates chromosome segregation in human cells. *J. Cell Sci.* 120:3748–3761. http://dx.doi.org/10.1242/jcs.009308

Torosantucci, L., M. De Luca, G. Guarguaglini, P. Lavia, and F. Degrassi. 2008. Localized RanGTP accumulation promotes microtubule nucleation at kinetochores in somatic mammalian cells. *Mol. Biol. Cell*. 19:1873–1882. http://dx.doi.org/10.1091/mbc.E07-10-1050

Tulu, U.S., C. Fagerstrom, N.P. Ferenz, and P. Wadsworth. 2006. Molecular requirements for kinetochore-associated microtubule formation in mammalian cells. *Curr. Biol.* 16:536–541. http://dx.doi.org/10.1016/j.cub.2006.01.060

van der Watt, P.J., C.P. Maske, D.T. Hendricks, M.I. Parker, L. Denny, D. Govender, M.J. Birrer, and V.D. Leaner. 2009. The Karyopherin proteins, Crm1 and Karyopherin beta1, are overexpressed in cervical cancer and are critical for cancer cell survival and proliferation. *Int. J. Cancer*. 124:1829–1840. http://dx.doi.org/10.1002/ijc.24146

Vetter, I.R., A. Arndt, U. Kutay, D. Görlich, and A. Wittinghofer. 1999. Structural view of the Ran-Importin beta interaction at 2.3 A resolution. *Cell*. 97:635–646. http://dx.doi.org/10.1016/S0092-8674(00)80774-6

Wiese, C., A. Wilde, M.S. Moore, S.A. Adam, A. Merdes, and Y. Zheng. 2001. Role of importin-beta in coupling Ran to downstream targets in microtubule assembly. *Science*. 291:653–656. http://dx.doi.org/10.1126/science.1057661

Wollman, R., E.N. Cytrynbaum, J.T. Jones, T. Meyer, J.M. Scholey, and A. Mogilner. 2005. Efficient chromosome capture requires a bias in the 'search-and-capture' process during mitotic-spindle assembly. *Curr. Biol.* 15:828–832. http://dx.doi.org/10.1016/j.cub.2005.03.019

Yaseen, N.R., and G. Blobel. 1999. GTP hydrolysis links initiation and termination of nuclear import on the nucleoporin nup358. *J. Biol. Chem.* 274:26493–26502. http://dx.doi.org/10.1074/jbc.274.37.26493

Zuccolo, M., A. Alves, V. Galy, S. Bolhy, E. Formstecher, V. Racine, J.B. Sibarita, T. Fukagawa, R. Shiekhattar, T. Yen, and V. Doye. 2007. The human Nup107-160 nuclear pore subcomplex contributes to proper kinetochore functions. *EMBO J.* 26:1853–1864. http://dx.doi.org/10.1038/sj.emboj.7601642